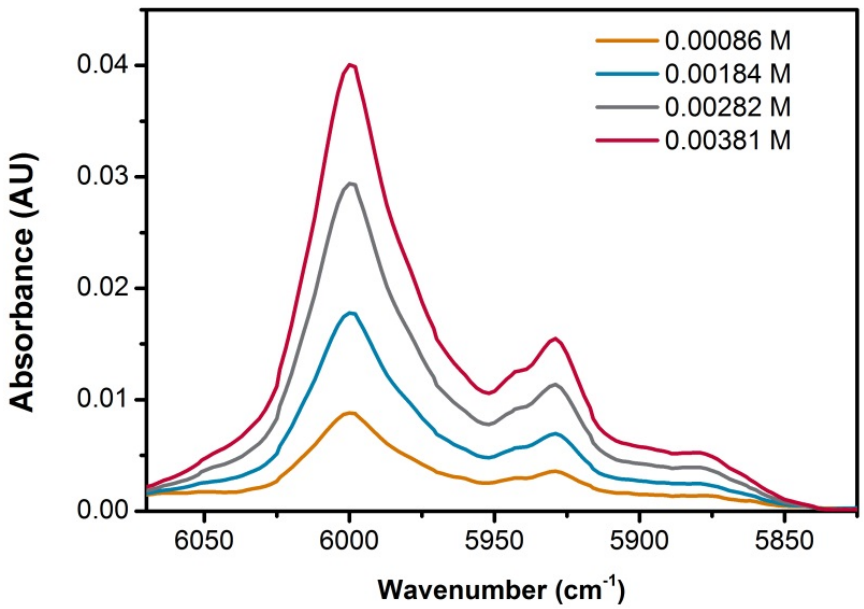

Mobilization and Transport of Organic Compounds from Geologic Carbon Sequestration Reservoirs

21 May 2015

Office of Fossil Energy

NRAP-TRS-III-002-2015

Disclaimer

This report was prepared as an account of work sponsored by an agency of the United States Government. Neither the United States Government nor any agency thereof, nor any of their employees, makes any warranty, express or implied, or assumes any legal liability or responsibility for the accuracy, completeness, or usefulness of any information, apparatus, product, or process disclosed, or represents that its use would not infringe privately owned rights. Reference therein to any specific commercial product, process, or service by trade name, trademark, manufacturer, or otherwise does not necessarily constitute or imply its endorsement, recommendation, or favoring by the United States Government or any agency thereof. The views and opinions of authors expressed therein do not necessarily state or reflect those of the United States Government or any agency thereof.

This report (PNNL-22791) has been reviewed by Pacific Northwest National Laboratory and approved for public release.

Cover Illustration: Representative benzene calibration data, near-infrared spectra of benzene in the CO_2 phase.

Suggested Citation: Cantrell, K. J; Zhong, L.; Bryce, D. A.; Thompson, C. J.; Bacon, D. H.; Shao, H. *Mobilization and Transport of Organic Compounds from Geologic Carbon Sequestration Reservoirs*; NRAP-TRS-III-002-2015; NRAP Technical Report Series; U.S. Department of Energy, National Energy Technology Laboratory: Morgantown, WV, 2015; p 54.

An electronic version of this report can be found at:

http://www.netl.doe.gov/research/on-site-research/publications/featured-technical-reports

https://edx.netl.doe.gov/nrap

Mobilization and Transport of Organic Compounds from Geologic Carbon Sequestration Reservoirs

K. J. Cantrell, L. Zhong, D. A. Bryce, C. J. Thompson, D. H. Bacon, H. Shao

Pacific Northwest National Laboratory, 902 Battelle Boulevard, Richland, WA 99354

NRAP-TRS-III-002-2015

Level III Technical Report Series

21 May 2015

This page intentionally left blank.

Table of Contents

EXECUTIVE SUMMARY **1**

1. INTRODUCTION **2**

2. MOBILIZATION OF ORGANIC COMPOUNDS FROM RESERVOIR ROCK AND CAPROCK AND TRANSPORT THROUGH SAND COLUMNS **3**
- 2.1 INTRODUCTION 3
- 2.2 MATERIALS AND METHODS 4
- 2.3 RESULTS 8
- 2.4 DISCUSSION 17
- 2.5 CONCLUSIONS 18

3. TRANSPORT OF ORGANIC CONTAMINANTS MOBILIZED BY $_{SC}CO_2$ FROM COAL THROUGH A SANDSTONE **19**
- 3.1 INTRODUCTION 19
- 3.2 MATERIALS AND METHODS 20
- 3.3 RESULTS 23
- 3.4 DISCUSSION 29

4. DETERMINATION OF ORGANIC PARTITIONING COEFFICIENTS IN WATER-SUPERCRITICAL CO_2 SYSTEMS BY SIMULTANEOUS IN SITU UV AND NEAR-INFRARED SPECTROSCOPIES **30**
- 4.1 INTRODUCTION 30
- 4.2 METHODS AND MATERIALS 31
- 4.3 RESULTS 35
- 4.4 DISCUSSION 40

5. REFERENCES **43**

List of Figures

Figure 1: Schematic of experimental setup used to study organic mobilization and transport (top). The flow lines were routed as indicated with red solid line during mobilization tests, and the red dashed line during column tests. The photograph shows the transport column test set up (bottom). 6

Figure 2: Ratio of VOC, PAH (naphthalene), and alkanes concentrations from Gothic shale by extracted $scCO_2$ over CH_2Cl_2: a) VOCs and naphthalene; b) alkanes. Benzene was not analyzed in this set of extraction. 10 g of rock sample was used in each test. The extraction conditions were 65°C and 1,500 psi. 10

Figure 3: Ratio of organic compound concentrations extracted by wet $scCO_2$ over dry $scCO_2$ from Gothic shale. Benzene was not analyzed in this set of extractions. The extraction conditions were 65°C and 10.3 MPa.....10

Figure 4: Concentrations of alkanes extracted by CH_2Cl_2 from Rock-1 (Desert Creek limestone) and its Caprock Rock-2 (Gothic shale). The extraction condition was 65°C and 1,500 psi. 11

Figure 5: BTEX and naphthalene concentrations extracted from Fruitland coal by water saturated $scCO_2$ as a function of reaction time at 65°C temperature and 1,500 psi pressure. 10 g of coal was used in each extraction. 12

Figure 6: Comparison of extractable organic compound concentrations for $scCO_2$ and methylene chloride from Fruitland coal at 65°C temperature and 1,500 psi pressure: a) VOCs and naphthalene; b) alkanes. 13

Figure 7: Column effluent gas organic compound concentrations normalized by inflow gas concentrations in dry column tests. Fruitland coal was used for organics mobilization: a) mobilized by dry $scCO_2$; b) mobilized by water saturated $scCO_2$.....14

Figure 8: Organic compound concentrations extracted by $scCO_2$ at 95°C and 1,500 psi pressure from Fruitland coal, Gothic shale, Teapot Dome sandstone. 15

Figure 9: Column effluent concentrations normalized by inflow concentrations in wet column tests. Organics were mobilized from: a) Fruitland coal (Col-3), b) Gothic shale (Col-4), and c) Teapot Dome sandstone (Col-5). Extraction conditions were 95°C and 1,500 psi. 16

Figure 10: Schematic of experimental setup. 21

Figure 11: Mass percent of organic compounds retained within the columns as a function of pressure (at 20°C). 25

Figure 12: Mass percent of organic compounds retained within the columns as a function of temperature at 1,000 psig.....25

Figure 13: BTEX compound concentration distribution in rock cores from Test CF-1 (20°C and ambient pressure). Rock cores were numbered No. 1 through No. 6 from the inflow end of the column. 26

Figure 14: Naphthalene concentration distribution in rock cores in Test CF-1 (20°C and ambient pressure). 27

Figure 15: Percent of retained organic compound mass in each core in the total retained mass for tests CF-1, 20°C and ambient pressure (a), and CF-3, 20°C and 1,000 psig (b). 27

Figure 16: Concentration of organic contaminants of pore water in the rock cores for Test CF-1 (20°C and ambient pressure). 28

Figure 17: CO_2 density as a function of pressure for the temperatures used in this study. Densities were calculated using the software program EOS-SCx. 32

Figure 18: Schematic of the high-pressure titration system with dual spectroscopic detectors. 33

Figure 19: Benzene spectra: (A) near-infrared spectrum of a 0.0046 M solution of benzene in the CO_2-rich phase (50°C and approximately 97 bar), and (B) UV spectrum of a 0.0054 M aqueous solution at ambient conditions (22°C and approximately 1 bar). 36

Figure 20: Representative benzene calibration data: (A) near-infrared spectra of benzene in the CO_2 phase, (B) plot of integrated near-infrared absorbance versus concentration, (C) UV spectra of benzene in water, and (D) Plot of UV absorbance at 254 nm versus concentration. 37

Figure 21: Concentrations of benzene in the aqueous and CO_2 phases after injecting benzene into the reactor. 38

Figure 22: Partitioning coefficients of benzene in water-CO_2 determined in this study. 39

Figure 23: Aqueous benzene concentrations as a function of CO_2 phase density. 40

List of Tables

Table 1: Rock Samples used in Mobilization and Transport Experiments 4

Table 2: Summary of Column Tests 7

Table 3: Organic Compounds Quantified in this Study 7

Table 4: Organic Compound Concentrations Extracted by CH_2Cl_2 from Rock Samples 9

Table 5: Organic Compound Concentrations Extracted from Fruitland Coal with $scCO_2$ 12

Table 6: Summary of Experiments for Organic Compound Transport through Rock Core 22

Table 7: Properties of Analyzed Compounds 23

Table 8: Mass percent of Organic Compounds Transported through the Column 24

Table 9: Benzene Partitioning Coefficients Determined in this Study 39

Table 10: Calculated Benzene Concentrations for a Theoretical System of Equal Volumes H_2O and CO_2 42

Acronyms, Abbreviations, and Symbols

Term	Description
Al	Aluminum
BTEX	Benzene, toluene, ethyl-benzene, xylene
CH_2Cl_2	Methylene chloride
CO_2	Carbon dioxide
DI	Deionized (water)
DOE	U.S. Department of Energy
EOR	Enhanced oil recovery
EPA	U.S. Environmental Protection Agency
GC-MS	Gas chromatography–mass spectroscopy
GCS	Geologic carbon storage
HPLC	High-performance liquid chromatography
ID	Inside diameter
MCL	Maximum contaminant level
NIRS	Near-infrared spectroscopy
NRAP	National Risk Assessment Partnership
OD	Outside diameter
PAH	Polycyclic aromatic hydrocarbon
PNNL	Pacific Northwest National Laboratory
$scCO_2$	Supercritical carbon dioxide
STOMP	Subsurface Transport Over Multiple Phases
UV	Ultraviolet
VOC	Volatile organic compound

Units of Measure

Term	Description
°C	Temperature in degrees Celsius
cm	Centimeter(s)
g	Gram(s)
h	Hour(s)
in.	Inch(es)
kg	Kilogram(s)
L	Liter(s)
M	Molar
m	Molal
m	Meter(s)
md	Millidarcy
mL	Milliliter
µm	Micrometer
min	Minute(s)
mg	Milligram(s)
mm	Millimeter(s)
MPa	Megapascal(s)
nm	Nanometer(s)
psi	Pounds per square inch
psig	Pounds per square inch gage
wt%	Weight percent

Acknowledgments

This work was completed as part of the National Risk Assessment Partnership (NRAP) project. Support for this project came from the U.S. Department of Energy (DOE) Office of Fossil Energy's Crosscutting Research program. This work was funded as part of the American Recovery and Reinvestment Act of 2009. The authors wish to acknowledge Traci Rodosta (Carbon Storage Technology Manager), Kanwal Majajan (Carbon Storage Division Director), M. Kylee Rice (Project Manager), Mark Ackiewicz (Division of CCS Research - Program Manager), Susan Maley and Steve Seachman (NETL Strategic Center for Coal), and Regis Conrad (DOE Office of Fossil Energy) for programmatic guidance, direction, and support.

The authors acknowledge technical reviews by N. P. Qafoku (Pacific Northwest National Laboratory) and word processing by K. R. Neiderhiser. This document has been entered into the PNNL information release system as document number PNNL-22791. Pacific Northwest National Laboratory is operated by Battelle Memorial Institute for the U.S. Department of Energy.

EXECUTIVE SUMMARY

This report summarizes results of research conducted during FY2012–FY2013 to support the assessment of environmental risks associated with geologic carbon dioxide (CO_2) sequestration and storage. Several research focus areas are ongoing as part of this project. This includes the quantification of the mobility of organic compounds and metals from representative CO_2 storage reservoir and caprock materials, the fate of organic compounds and metals after release, and the development of a method to measure pH in situ under supercritical CO_2 ($scCO_2$) conditions. This report focuses specifically on results for organic compounds.

Experiments have been conducted to evaluate the potential for mobilization of organic compounds from representative reservoir materials and caprock and their fate in porous media (quartz sand). Results with Fruitland coal and Gothic shale indicate that lighter organic compounds were more susceptible to mobilization by $scCO_2$ compared to heavier compounds. Alkanes demonstrated very low extractability by $scCO_2$. No significant differences were observed between the extractability of organic compounds by dry or water saturated $scCO_2$. Reaction equilibrium appears to have been reached by 96 hours.

When the $scCO_2$ was released from the reactor, less than 60% of the injected lighter compounds (benzene, toluene) were transported through the dry sand column by the CO_2, while more than 90% of the heavier organics were trapped in the sand column. For wet sand columns, most (80–100%) of the organic compounds injected into the sand column passed through, except for naphthalene which was substantially removed from the CO_2 within the column.

In addition to the column experiments conducted with quartz sand, column experiments were also conducted using a wetted sandstone rock installed in a tri-axial core holder to study the flow and transport of organic compounds mobilized by $scCO_2$ under simulated geologic carbon storage (GCS) conditions. The sandstone rock was collected from a formation overlying a deep saline reservoir at a GCS demonstration site. Rock core effluent pressures were set at 0, 500, or 1,000 psig and the core temperature was set at 20°C or 50°C to simulate the transport to different subsurface depths. The concentrations of the organic compounds in the column effluent and their distribution within the sandstone core were monitored. Results indicate that the mobility though the core sample was much higher for benzene, toluene, ethylbenzene, and xylenes than for naphthalene. Retention of organic compounds from the vapor phase to the core appeared to be primarily controlled by partitioning from the vapor phase to the aqueous phase. Adsorption to the surfaces of the wetted sandstone was also significant for naphthalene. Reduced temperature and elevated pressure resulted in greater partitioning of the mobilized organic contaminants into the water phase.

1. INTRODUCTION

Injection of carbon dioxide (CO_2) into deep subsurface reservoirs for permanent storage or sequestration has the potential to mobilize organic and metal contaminants from storage reservoir materials and overlying caprock. Organic and metal contaminants can leach into the brine phase in these reservoirs, and organic contaminants can dissolve into the $scCO_2$ phase. If either of these phases were to escape the storage reservoir through fractures or faults in the caprock or through faulty wells that penetrate the reservoir, it could potentially result in the contamination of overlying aquifers.

This work is supported by the National Risk Assessment Project (NRAP) and has three primary objectives. The first is to determine the rates and mechanisms that govern contaminant migration from reservoir and caprock materials into the brine and $scCO_2$ phases within the CO_2 storage reservoirs. The second is to determine the fate of these contaminants during migration of contaminated brine and $scCO_2$ phases from the storage reservoir through overlying rock layers to an overlying aquifer during a hypothetical leak from the reservoir. The third is to determine the impact of various leakage scenarios on overlying groundwater aquifers.

This report summarizes research conducted during FY2012–FY2013 to support the NRAP objectives for organic contaminants. This report is organized into sections that cover specific tasks completed as part of the project. Section 2 describes results of experiments to quantify the mobilization of organic compounds from representative reservoir rock and caprock samples by $scCO_2$ and subsequent transport through sand columns. In Section 3, results from experiments to quantify transport of organic contaminants mobilized from coal through sandstone core are presented. Section 4 describes an advanced method for determining partitioning coefficients of organic contaminants between $scCO_2$ and brine and presents the initial results using this method focusing primarily on benzene.

2. MOBILIZATION OF ORGANIC COMPOUNDS FROM RESERVOIR ROCK AND CAPROCK AND TRANSPORT THROUGH SAND COLUMNS

2.1 INTRODUCTION

Geological carbon storage (GCS) is one of the primary options for long-term storage of anthropogenic CO_2 in the deep subsurface to minimize increased CO_2 concentrations in the atmosphere and constrain global warming (Bachu, 2000; Bachu and Adams, 2003; White et al., 2003). Concerns regarding the potential for groundwater contamination by toxic organic compounds mobilized from GCS sites have been raised (Xu et al., 2007; Kharaka et al., 2009). Depleted oil reservoirs and deep saline aquifers have been proposed as sites for CO_2 storage. The organic content of depleted oil reservoir rock can be high due to residual petroleum. Non-oil-bearing saline aquifers can also be a source of toxic organic compounds during $scCO_2$ injection (Kharaka et al., 2006).

Under the pressure and temperature conditions of GCS storage reservoirs, CO_2 occurs as a supercritical phase. Supercritical CO_2 ($scCO_2$) is an excellent solvent for organic compounds (Anitescu and Tavlarides, 2006; Kolak and Burruss, 2006). Benzene, toluene, ethyl-benzene, xylene (BTEX), phenol, and polycyclic aromatic hydrocarbon (PAH) compounds can be effectively solubilized into $scCO_2$. Toxic organic compounds can dissolve into $scCO_2$ during carbon storage, and if a CO_2 leak were to occur, the organic compounds could be transported into overlying aquifers (Apps et al., 2010). Groundwater monitoring results from GCS test sites have shown increased organic compound concentrations after CO_2 injection (Scherf et al., 2011; Kharaka et al., 2009, 2010b, 2011). The risk of groundwater contamination by toxic organic constituents mobilized by $scCO_2$ injection at GSC sites and subsequent transport to shallow drinking water aquifers via leakage pathways must be addressed in order to gain public acceptance of CO_2 injection. Knowledge of the mobilization mechanisms of organic compounds and their transport and fate in the subsurface is essential for assessing risks associated with GCS.

Numerous studies over the past 30 years have demonstrated the mobilization of organic matter from oil shales, sediment rocks, siltstone, and coals by $scCO_2$ (McKay and Chong, 1983; Qin et al., 1984; Monin et al., 1988; Jaffé et al., 1997, 2000; Olukcu et al., 1999; Koel and Ljovin, 2000; Akinlua et al., 2008; Okamoto et al., 2005; Kolak and Burruss, 2006; Scherf et al., 2011). Most of these studies were focused on extraction efficiency for hydrocarbon recovery; however, Akinlua et al. (2008) studied the kinetics of extraction and Jaffé et al. (2000) reported on the influence of temperature. Only a few recent studies were focused on the potential for organic matter mobilization by $scCO_2$ injection during GCS (Kolak and Burruss, 2006; Scherf et al., 2011) or the potential for organic mobilization to impact the sealing performance of storage reservoir caprock (Okamoto et al., 2005). No investigations on the kinetics and extent of toxic organic constituent mobilization by $scCO_2$ from reservoir rocks have been reported.

Studies on subsurface transport and fate of organic compounds with CO_2 are sparse. Zheng et al. (2010) conducted modeling studies regarding the transport of mobilized benzene and co-injected inorganic gases in GCS systems. Phase partitioning between benzene, water, and the $scCO_2$ phase was considered as the major controlling factor in the transport of the organic compounds. When $scCO_2$ leaks from the GCS reservoir, CO_2 will transform into the gas phase as it rises through the geologic strata and temperature and pressure are reduced. No investigations have

been reported on subsurface transport of mobilized organic compounds in gas phase CO_2 at this time.

In this study, mobilization of organic compounds by $scCO_2$ was investigated using rock samples obtained from sites across the United States that are being developed or planned for geological carbon sequestration. These sites have been operated for enhanced oil recovery (EOR) or enhanced coal-bed methane recovery by CO_2 injection. The compounds studied were volatile organic compounds (VOCs), including BTEX, propylbenzene, 1,3,5-trimethylbenzene; naphthalene (a PAH); and n-alkanes (n-C20 – n-C30). The kinetics of mobilization of organic compounds by dry $scCO_2$ and water vapor saturated $scCO_2$ was studied. The organic compounds that could be mobilized by $scCO_2$ were compared with those that were extractable by methylene chloride (CH_2Cl_2). Column experiments were applied to study the transport characteristics of organic compounds mobilized by $scCO_2$.

2.2 MATERIALS AND METHODS

2.2.1 Materials

Six rock samples were used in the organic compound mobilization and transport experiments. These rock samples were collected from locations being tested or proposed as GCS sites. The locations and the descriptions of the rock samples are summarized in Table 1.

Table 1: Rock Samples used in Mobilization and Transport Experiments

Sample No.	Rock Name	Location; Depth (ft)	Lithology	Operation Performed
Rock-1	Desert Creek limestone	Aneth Oil Field, Utah; 5,398–5,404	Limestone	CO_2 enhanced oil recovery
Rock-2	Gothic shale	Aneth Oil Field, Utah; 5,390–5,394	Shale; Caprock for Desert Creek limestone	NA
Rock-3	Fruitland coal	Pump Canyon Site, New Mexico; 3,893	Coal	Enhanced coal-bed methane recovery by CO_2 injection.
Rock-4	Kirtland shale	Pump Canyon Site, New Mexico	Shale; Caprock formation for Fruitland coal	NA
Rock-5	Teapot Dome sandstone	Teapot Dome, Wyoming; 5,409	Sandstone	CO_2 enhanced oil recovery
Rock-6	Goose Egg shale	Teapot Dome, Wyoming; 5,300–5,400	Shale; Caprock for Tensleep sandstone	NA

NA = Not applicable

2.2.2 Methods

Methylene chloride (CH_2Cl_2) extractions were used as a baseline for comparison with $scCO_2$ extractions. Rock samples were prepared for CH_2Cl_2 extraction by crushing rock and sieving particles to less than 1.0 mm. Five grams of rock particles were added to a vial with 30 mL of CH_2Cl_2. The vials were sealed and place on a rotational mixer for 7 days (kinetic studies showed that extraction equilibrium was reached at 24 h). At the end of extraction, the mixture was centrifuged to separate the rock particles from the extractant, and organic compound concentrations in the CH_2Cl_2 were quantified by gas chromatography-mass spectrometry (GS-MS).

The experimental setup for the study of organic compound mobilization and transport by $scCO_2$ is shown schematically in Figure 1. In the mobilization tests, a Parr reactor (100 mL) with a heat jacket and temperature control system was used to extract the rocks with $scCO_2$. Either 10 g or 15 g of rock sample with particle size of <1.0 mm was used for the extractions. No water was added to the sample for dry $scCO_2$ mobilization tests. For water saturated $scCO_2$ extractions, a vial containing 0.5 mL of deionized (DI) water was placed in the reactor with the rock sample. Based on the water solubility in $scCO_2$ (Spycher et al., 2003), the $scCO_2$ was saturated with water at the test conditions for all the experiments. An ISCO syringe pump was used to pressurize and charge the reactor with CO_2. The pressure and temperature were adjusted to desired values and monitored over the course of the experiment. A needle valve was used to control the flow rate of CO_2 released from the reactor during sampling. The released gas was directed through two CH_2Cl_2 traps where organic compounds mobilized by the $scCO_2$ were extracted by the solvent. A flow meter was used to measure the gas flow rate. A pressure monitor system installed on the reactor was used to record pressure changes during sampling. Stainless steel tubing (0.125 in. outside diameter [OD]) was used to connect the reactor with the CH_2Cl_2 traps. The tubing was heated to 97°C during sampling to minimize condensation of organic compounds. After the extraction process, the tubing was flushed with CH_2Cl_2 to extract and quantify the organic compounds that could have potentially condensed in the tubing during sampling. The pressures and temperatures before and after sampling were used to calculate the CO_2 mass released from the reactor during sampling.

In the column tests, CO_2 gas containing mobilized organics was released from the reactor and injected through a column (2.54 cm inside diameter [ID] by 10 cm L) packed with 20/30 Accusand (Figure 1). This sand had narrow particle size distribution, with a median particle diameter of 0.713 mm and a standard deviation of 0.023 mm (Schroth et al., 1996). Tests were performed with dry sand and with wet, but unsaturated, sand. The wet sand column was established by first saturating the column with DI water, and then draining the column under ambient conditions. The gas effluent from the column was directed through two CH_2Cl_2 traps (Figure 1) and then vented to the atmosphere through a flow meter. When the gas flow was completed, the organic compounds that condensed on the sand were extracted with CH_2Cl_2 by mixing the sand with the solvent in a glass bottle. The stainless steel tubing (0.0125 in. OD) used to connect the reactor and the column was heated during the experiment and flushed with CH_2Cl_2 to quantify and condense compounds as described previously. The concentrations of organic compounds trapped in the sand and in the column effluent were quantified. A total of five column experiments were conducted, as summarized in Table 2.

An Agilent Technologies 5975C GC-MS system was used for organic compound identification and quantification. An Agilent capillary column (0.25 mm × 30 m × 0.25 μm) was used to

separate the organic compounds. Commercial standards were used for calibration of the GC-MS. The temperature for the GC column was initially set at 32°C, held for 2 min and then ramped up at 5°C/min to 280°C, and then held at this temperature for 5 min. A set of VOCs, semi-volatile organic compounds (semi-VOCs), and n-alkanes were identified and quantified using this method. Organic compounds such as BTEX and naphthalene were of primary interest, but other VOCs such as iso-propylbenzene, propylbenzene, and 1,3,5-trimethylbenzene, etc., and n-alkanes (n-C20 – n-C30) were included in the study. For reference, the list of the compounds including their maximum contaminant levels (MCLs) allowable in drinking water are shown in Table 3.

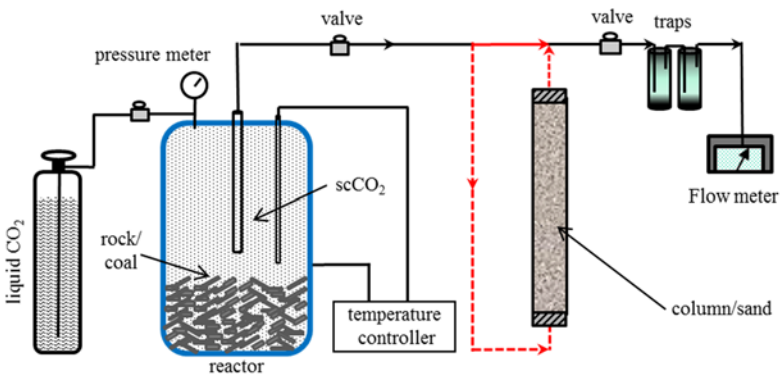

Figure 1: Schematic of experimental setup used to study organic mobilization and transport (top). The flow lines were routed as indicated with red solid line during mobilization tests, and the red dashed line during column tests. The photograph shows the transport column test set up (bottom).

Table 2: Summary of Column Tests

Test Name	Description Packing; Wet/Dry $scCO_2$; Effluent P	Rock for Extraction	P(psi)/T(°C)	Sampling Approach
Col-1	Dry Accusand; Dry CO_2	Fruitland coal	1,500/65	2 CH_2Cl_2 traps in effluent; sand extracted with CH_2Cl_2
Col-2	Dry Accusand; Wet CO_2	Fruitland coal	1,500/95	2 CH_2Cl_2 traps in effluent; sand extracted with CH_2Cl_2
Col-3	Wetted Accusand; Wet CO_2	Fruitland coal	1,500/95	2 CH_2Cl_2 traps in effluent; sand and water extracted with CH_2Cl_2
Col-4	Wetted Accusand; Wet CO_2	Gothic shale	1,500/95	2 CH_2Cl_2 traps in effluent; sand and water extracted with CH_2Cl_2
Col-5	Wetted Accusand; Wet CO_2	Tensleep sandstone	1,500/95	2 CH_2Cl_2 traps in effluent; sand and water extracted with CH_2Cl_2

Table 3: Organic Compounds Quantified in this Study

Chemical Name	Formula	MCL (mg/L)
Benzene	C_6H_6	0.005
Toluene	C_7H_8	1.0
Ethylbenzene	C_8H_{10}	0.7
m-Xylene + p-Xylene	C_8H_{10}	10 (total)
o-Xylene		
Iso-Propylbenzene	C_9H_{12}	NA
Propylbenzene	C_9H_{12}	NA
1,3,5-Trimethylbenzene	C_9H_{12}	NA
1,2,4-Trymethylbenzene	C_9H_{12}	NA
Tert-butyl-Benzene	$C_{10}H_{14}$	NA
Sec-Butylbenzene	$C_{10}H_{14}$	NA
p-Isopropyltoluene	$C_{10}H_{14}$	NA
Butylbenzene	$C_{10}H_{14}$	NA
Naphthalene	$C_{10}H_8$	NA (possible human carcinogen)
n-Decane	$C_{10}H_{22}$	NA
n-Icosane	$C_{20}H_{42}$	NA
n-Docosane	$C_{22}H_{46}$	NA
n-Tetracosane	$C_{24}H_{50}$	NA
n-Hexacosane	$C_{26}H_{54}$	NA
n-Octacosane	$C_{28}H_{58}$	NA
n-Triacontane	$C_{30}H_{62}$	NA

NA = Not applicable

2.3 RESULTS

2.3.1 Methylene Chloride Extractable Organic Compounds

The CH_2Cl_2 extractable organic compound concentrations of the rock samples were used as a baseline for comparison with the organic compounds mobilized by $scCO_2$. The measured organic compound concentrations in CH_2Cl_2 were used to calculate the extracted concentrations from the rock samples (in mg/kg-rock) based on mass balance. The extracted concentrations for the various rock samples used in this study are listed in Table 4. Rock-3 (Fruitland coal) showed the highest extractable VOC and PAH concentrations, followed by Rock-2 (Gothic shale) and Rock-1 (Desert Creek limestone). The other rock samples showed very low extractable organic compound concentrations. Rock-4 (Kirtland shale) had the highest extractable n-alkane concentrations, followed by Rock-3, Rock-5, Rock-1, Rock-2, and Rock-6. The results for the rock samples from the EOR sites (Rock-1 and Rock-5) were much lower than expected, particularly for the lighter compounds. It is likely that the lighter compounds that remained in these samples after EOR had volatilized during storage. These samples had been stored for years in a warehouse with no special precautions to preserve their volatile organic compound content. As a result, the extractable organic compound content determined for these samples is not likely to be representative of that in depleted oil reservoir rock that would occur in situ.

The focus of this study was on the mobilization of VOCs and naphthalene. Therefore, Rock-3 and Rock-2 were used primarily in subsequent experiments because of their relative higher concentrations of these compounds.

Table 4: Organic Compound Concentrations Extracted by CH_2Cl_2 from Rock Samples (mg/kg-rock)

Organic Compound	Rock-1 Desert Creek Limestone	Rock-2 Gothic Shale	Rock-3 Fruitland Coal	Rock-4 Kirtland Shale	Rock-5 Tensleep Sandstone	Rock-6 Goose Egg Shale
Benzene	N.A.	1.6	113.4	0.5	0.4	0.1
Toluene	1.6	4.62	210.0	0.4	0.4	0.1
Ethylbenzene	0.0	2.28	5.3	0.0	0.0	0.0
Xylene (m&p)	0.0	4.14	98.3	0.0	0.0	0.0
Xylene (o)	0.0	4.92	83.6	0.0	0.0	0.0
Isopropylbenzene	0.0	1.02	1.7	0.0	0.0	0.0
Propylbenzene	0.0	1.56	4.3	0.0	0.0	0.0
1,3,5-Trimethylbenzene	0.0	2.88	24.0	0.0	0.0	0.0
Tert-Butylbenzene	0.0	1.32	8.16	0.0	0.0	0.0
1,2,4-Trimethylbenzene	0.1	10.26	64.3	0.0	0.0	0.0
Sec-Butylbenzene	0.0	1.08	1.9	0.0	0.0	0.0
P-Isopropyltoluene	0.0	0.54	1.0	0.0	0.0	0.0
Butylbenzene	0.0	1.20	2.4	0.0	0.0	0.0
Naphthalene	0.6	2.34	99.3	0.0	0.0	0.0
n-Decane ($C_{10}H_{22}$)	1.1	39.5	282.06	0.5	0.3	0.0
n-Icosane ($C_{20}H_{42}$)	68.1	69.5	487.32	10.3	193.3	0.0
n-Docosane ($C_{22}H_{46}$)	100.1	48.5	629.70	700.7	188.3	0.1
n-Tetracosane ($C_{24}H_{50}$)	100.7	27.4	808.98	1,436.5	192.4	0.4
n-Haxacosane ($C_{26}H_{54}$)	83.0	21.1	782.10	1256.9	164.4	0.2
n-Octacosane ($C_{28}H_{58}$)	56.2	14.3	602.58	788.0	141.0	0.4
n-Triacontane ($C_{30}H_{62}$)	56.7	13.9	293.94	459.8	105.6	0.0
Total extracted/measured organic compounds	**468.2**	**273.9**	**4,604.4**	**4,653.6**	**986.3**	**1.3**

N.A. = Not analyzed

2.3.2 Mobilization from Gothic Shale (Rock-2) by $scCO_2$

The extractability of organic compounds by $scCO_2$ was determined by batch extraction for 7 days at 65°C and 1,500 psi. The extraction equilibrium was reached at about 100 h (see Figure 5). Ratios of the $scCO_2$ extractable organic compound concentrations relative to the CH_2Cl_2 extractable concentrations are shown in Figure 2. Both dry and water-saturated $scCO_2$ extracted more VOCs and naphthalene from the shale compared to the CH_2Cl_2 extraction, while n-C10 and n-C20 alkanes were much less extractable by $scCO_2$ than by CH_2Cl_2. Alkanes with 22 and higher carbons were not mobilized by $scCO_2$. This is consistent with the general trend of decreasing solubility of organic compounds in $scCO_2$ with increasing carbon number (Burant et al., 2013).

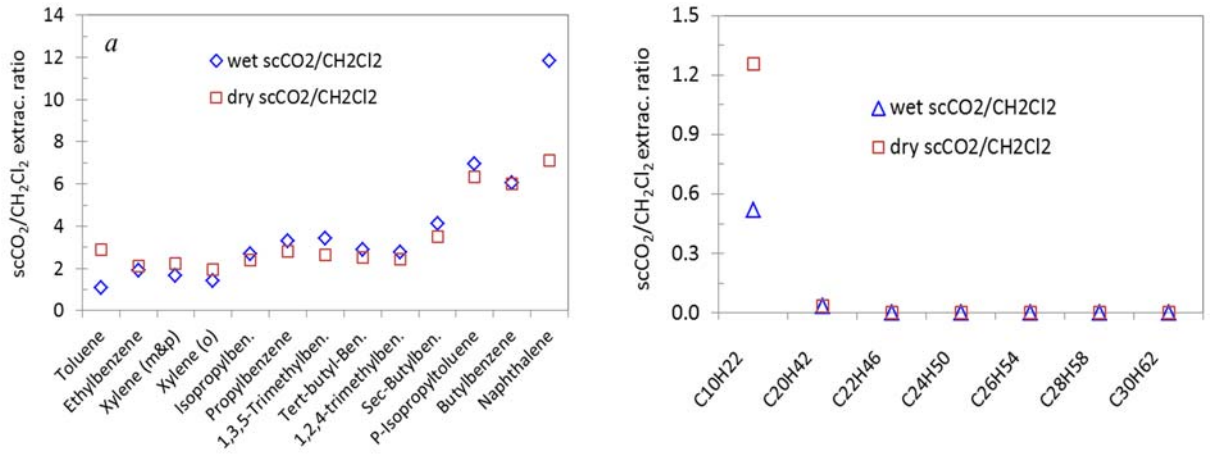

Figure 2: Ratio of VOC, PAH (naphthalene), and alkanes concentrations from Gothic shale by extracted $scCO_2$ over CH_2Cl_2: a) VOCs and naphthalene; b) alkanes. Benzene was not analyzed in this set of extraction. 10 g of rock sample was used in each test. The extraction conditions were 65°C and 1,500 psi.

Ratios of organic compounds mobilized from Gothic shale by water saturated $scCO_2$ over dry $scCO_2$ are shown in Figure 3. The differences in the extractability of most of the organic compounds for water saturated $scCO_2$ and dry $scCO_2$ is relatively small; however, significantly less (0.37 times) toluene was mobilized by water saturated $scCO_2$ than dry $scCO_2$, and significantly more (1.6 times) naphthalene was mobilized by water saturated $scCO_2$ than dry $scCO_2$.

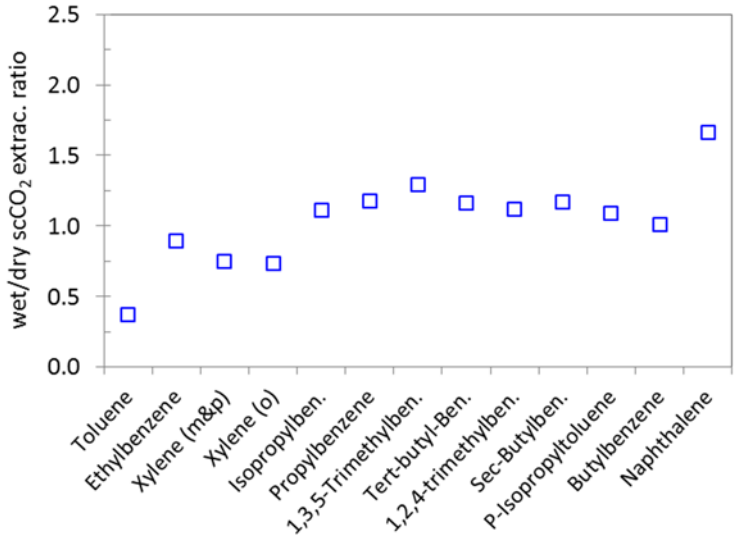

Figure 3: Ratio of organic compound concentrations extracted by wet $scCO_2$ over dry $scCO_2$ from Gothic shale. Benzene was not analyzed in this set of extractions. The extraction conditions were 65°C and 10.3 MPa.

A comparison of the CH_2Cl_2 extractable n-alkane concentrations from the Rock-1 (Desert Creek limestone) and its caprock Rock-2 (Gothic shale) is shown in Figure 4. From the depleted oil reservoir limestone, a very low concentration of $C_{10}H_{22}$ was extracted, while $C_{20}H_{42}$ and alkanes with higher carbon numbers showed much higher relative concentrations. These results are consistent with preferential extraction of the lighter organic components relative to the heavier components during EOR with $scCO_2$ and known solubility characteristics of organic compounds in $scCO_2$ (Hawthorne et al., 1994).

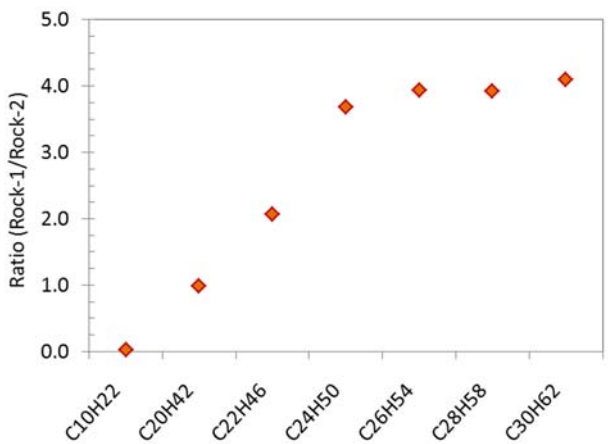

Figure 4: Concentrations of alkanes extracted by CH_2Cl_2 from Rock-1 (Desert Creek limestone) and its Caprock Rock-2 (Gothic shale). The extraction condition was 65°C and 1,500 psi.

2.3.3 Mobilization from Fruitland Coal (Rock-3) by $scCO_2$

The concentrations of organic compounds extracted from the Fruitland coal by dry and water saturated $scCO_2$ at 65°C and 1,500 psi are presented in Table 5. No significant differences were observed between the organic compound concentrations mobilized by dry and water saturated $scCO_2$. The concentrations of organic compounds extracted from Fruitland coal by water saturated $scCO_2$ as a function of time is shown in Figure 5. These results indicate that steady state for extraction was reached at or before 96 h.

Table 5: Organic Compound Concentrations Extracted from Fruitland Coal with $scCO_2$ (pressure = 1,500 psi and 65°C)

Compounds	Water-Saturated $scCO_2$ Concentration ($mg/kg\text{-}scCO_2$)			Dry $scCO_2$ Concentration ($mg/kg\text{-}scCO_2$)		
	24 h	96 h	216 h	24 h	96 h	216 h
Benzene	37.2	61.0	59.9	36.8	44.9	64.8
Toluene	69.5	105.0	108	90.1	91.8	133
Ethylbenzene	1.77	1.92	2.36	1.87	2.13	2.98
m-Xylene + m-Xylene	24.2	35.4	35.9	26.5	33.6	45.2
o-Xylene	11.2	13.9	15.6	19.3	22.0	30.4
Iso-propylbenzene	0.00	0.00	0.00	0.00	0.22	0.00
Propylbenzene	0.65	0.79	0.44	0.00	0.37	0.89
1,3,5-Trimethylbenzene	1.32	1.07	0.65	2.96	5.18	6.29
1,2,4-Trimethylbenzene	3.85	6.41	7.32	8.09	9.81	10.3
Tert-Butylbenzene	1.25	2.33	2.81	0.73	0.44	0.40
Sec-Butylbenzene	0.88	1.88	2.33	0.15	0.00	0.34
p-Isopropyltoluene	0.00	0.00	0.00	0.00	0.19	0.00
Butylbenzene	0.00	0.00	0.00	0.25	0.00	0.00
Naphthalene	1.79	3.28	3.27	4.76	3.18	4.76

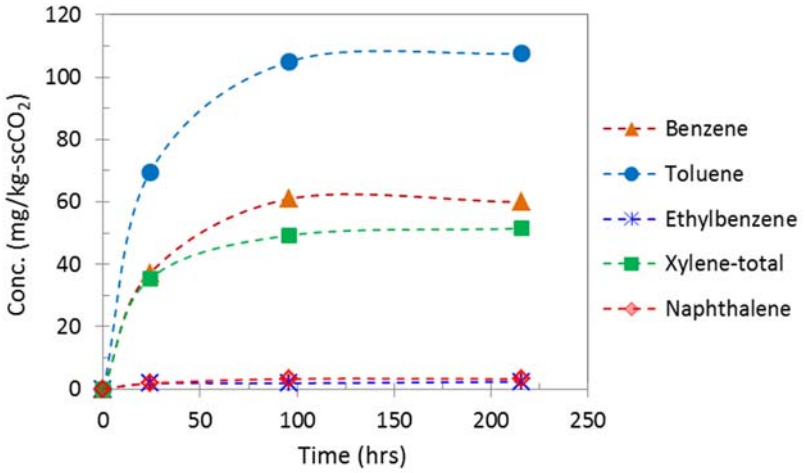

Figure 5: BTEX and naphthalene concentrations extracted from Fruitland coal by water saturated $scCO_2$ as a function of reaction time at 65°C temperature and 1,500 psi pressure. 10 g of coal was used in each extraction.

Figure 6 shows the ratio of organic compound concentrations extracted from Fruitland coal by $scCO_2$ over by CH_2Cl_2 at 65°C and 1,500 psi. For nearly all the compounds, only a fraction of the CH_2Cl_2 extractable organic compounds were extracted by $scCO_2$. The lighter compounds were more susceptible to extraction by $scCO_2$ than the heavier compounds. With the exception of $C_{10}H_{22}$, n-alkanes were not extracted by $scCO_2$.

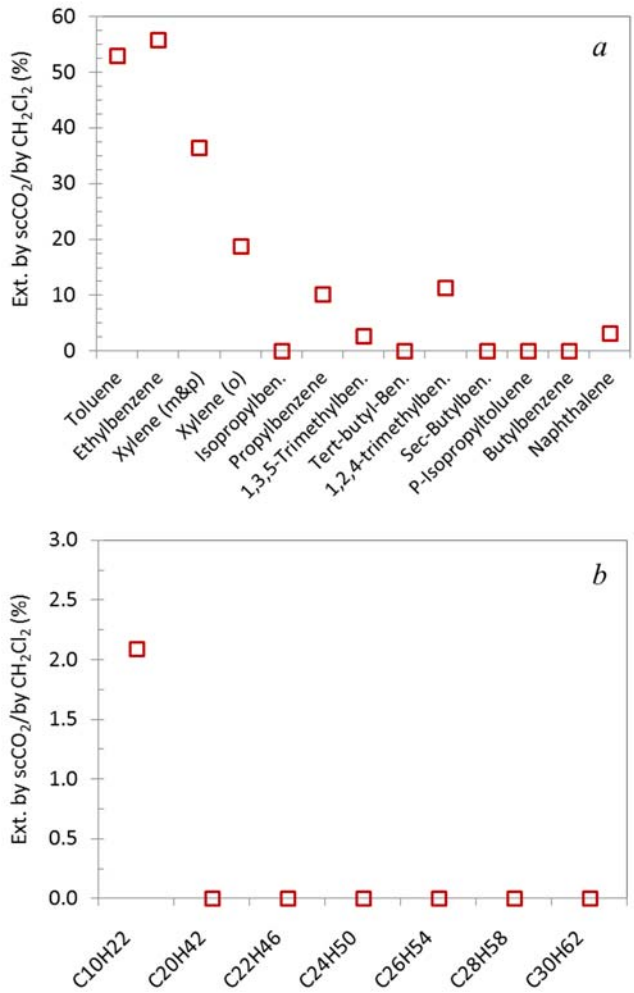

Figure 6: Comparison of extractable organic compound concentrations for $scCO_2$ and methylene chloride from Fruitland coal at 65°C temperature and 1,500 psi pressure: a) VOCs and naphthalene; b) alkanes.

2.3.4 Transport and Fate of Mobilized Organic Compounds

Transport of Organic Compounds through Dry Sand Columns

In dry sand columns (Table 2) the organic compound concentrations in the column effluent gas were normalized by the column inflow gas concentrations (Figure 7). The organic compounds were mobilized from Rock 3 (Fruitland coal) by dry (Figure 7a) or water saturated (Figure 7b) $scCO_2$ at 65°C and 1,500 psi. More than 40% of the lighter compounds (benzene, toluene) traveled through the sand column with the CO_2 gas (less than 60% was sorbed or condensed onto the dry sand in the column); while typically more than 90% of the heavier organics were trapped in the dry sand pack. The transport behavior of organic compounds mobilized by dry and water saturated $scCO_2$ through the dry sand columns were very similar (Figure 7a vs. 7b).

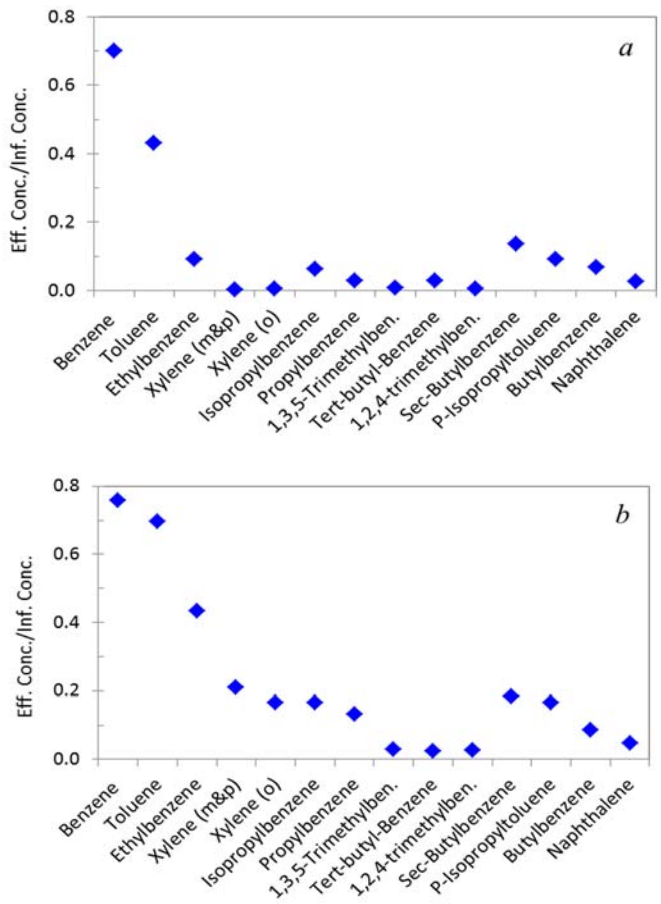

Figure 7: Column effluent gas organic compound concentrations normalized by inflow gas concentrations in dry column tests. Fruitland coal was used for organics mobilization: a) mobilized by dry $scCO_2$; b) mobilized by water saturated $scCO_2$.

Transport of Organic Compounds through Wet Sand Columns

Organic transport experiments through wet sand columns (see Table 2) were conducted using organic compounds extracted from three source rocks (Fruitland coal, Gothic shale, Teapot Dome sandstone) at 95°C temperature and 1,500 psi pressure. The concentrations of organic compounds in the $scCO_2$ extracted from the three rock samples used for the column experiments are shown in Figure 8. There are large concentration differences among the rocks. For the majority of the compounds, the extractable concentrations from Fruitland coal were between 2 and 25 times higher than those from Gothic shale, and were between 5 to 200 times higher than those from the Teapot Dome sandstone. The total quantified VOCs and PAH extracted from Fruitland coal was about 10 and 100 times of that extracted from the Gothic shale and Teapot Dome sandstone, respectively. The low organic compound concentrations mobilized from the Tensleep sandstone may be due to the fact that these samples were stored in a manner that would not prevent volatilization of organic compounds. Note how the difference in the quantity of mobilized organic compounds among the three samples decreased with increasing molecular weight of the organic compounds.

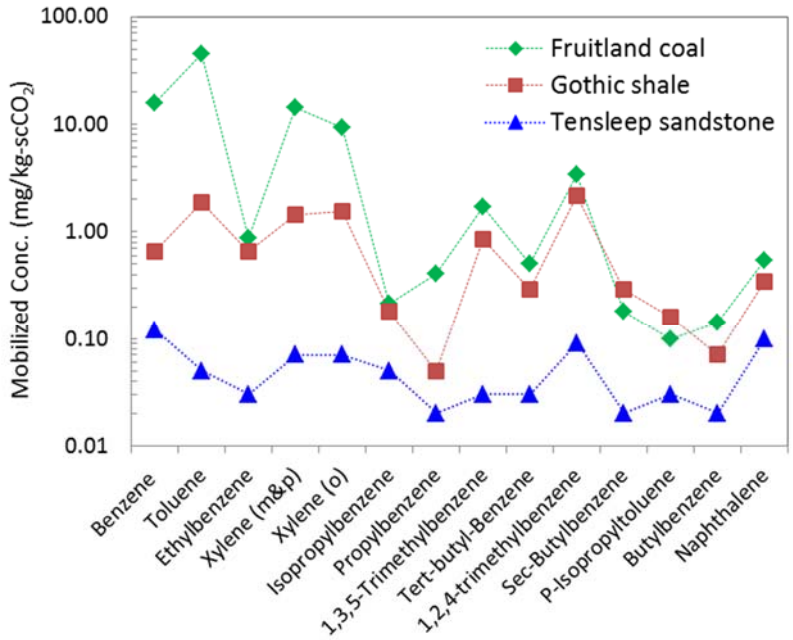

Figure 8: Organic compound concentrations extracted by $scCO_2$ at 95°C and 1,500 psi pressure from Fruitland coal, Gothic shale, Teapot Dome sandstone.

Results for organic compound transport through the wet sand columns are shown in Figure 9. The organic compound concentrations in the column effluent gas were normalized by the column inflow gas concentrations. Results indicate that the majority (>82%) of the organic compounds moved through the wet sand (with 13.7% water) columns, with the exception of naphthalene. Only 16% of naphthalene was transported through the wet sand column. The mass percentage of the organic compounds that moved through the columns was similar for all three source rocks, despite the remarkable differences in the total organic compound concentrations that were mobilized (Figure 8). For most of the compounds in test Col-5 (Table 2), close to 100% was transported through the column (Figure 9c). It is possible that some very low level concentrations of these compounds were trapped in the sand, but were below the quantification limit of the applied analytical approach.

Moisture in the sand column had a dramatic influence on the transport behavior of the organic compounds through the column. The observed differences in the mobility of the organic compounds between the dry and moist sand columns was presumably due to the hydrophobic nature of the compounds. The presence of a layer of water on the sand grains dramatically reduced the ability of the sand to adsorb organics compounds, greatly reducing the retardation of the VOC compounds and naphthalene (Cabbar and Bostanci, 2001; Ruiz et al., 1998).

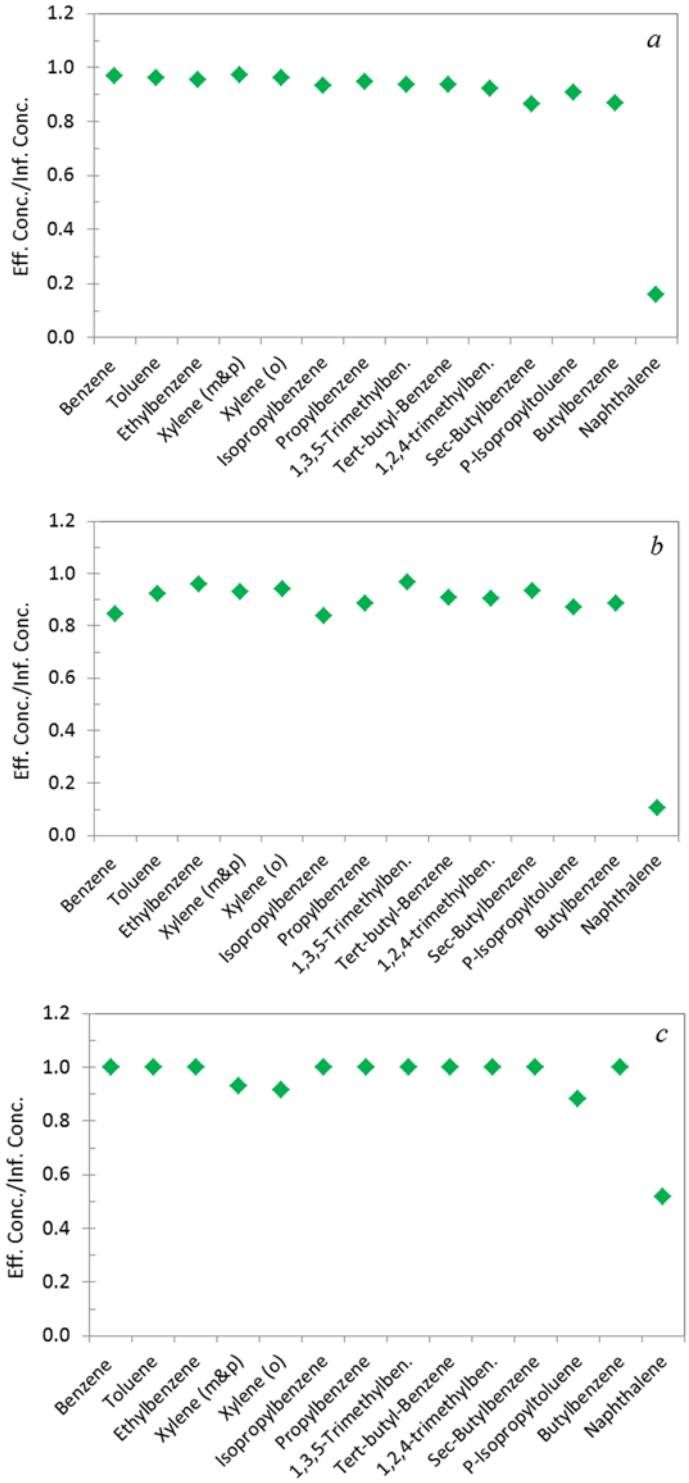

Figure 9: Column effluent concentrations normalized by inflow concentrations in wet column tests. Organics were mobilized from: a) Fruitland coal (Col-3), b) Gothic shale (Col-4), and c) Teapot Dome sandstone (Col-5). Extraction conditions were 95°C and 1,500 psi.

2.4 DISCUSSION

This section describes the results for organic compounds extracted from Fruitland coal by $scCO_2$ evaluated in the context of a CO_2 storage reservoir leak scenario and the potential impact of mobilized organic compounds on an overlying aquifer. This preliminary and simplistic analysis used parameters consistent with a simulated leak from a CO_2 storage reservoir modeled by Fahrner et al. (2012). In that model scenario, a leak of 23.7 tons of CO_2 is intruded into the bottom of an aquifer within an area of 150 m × 50 m over the course of 1 yr. The aquifer is assumed to be 10 m thick, with a porosity of 0.3. The volume of water contained within this area of the aquifer is equal to 2.25×10^7 L. Using the concentrations of benzene and naphthalene measured in the $scCO_2$ extracted from Fruitland coal from Figure 9, the total quantities of these compounds in the 23.7 tons of CO_2 was determined to be 370 g benzene and 12.8 g naphthalene. Assuming all the benzene and naphthalene in the CO_2 dissolves into the water contained within the model domain, the resulting concentrations were 16.4 µg/L benzene and 0.57 µg/L naphthalene. For comparison the U.S. Environmental Protection Agency (EPA) MCL for benzene is 5µg/L and 0.2 µg/L for PAHs [benzo(a)pyrene](EPA, 2012).

Although the dissolved concentrations of benzene and naphthalene calculated in this simple model are somewhat above their respective MCLs, a number of processes that were not accounted for could reduce the actual concentrations that would occur in the aquifer. These include adsorption, dilution, dispersion, and biodegradation. Adsorption to mineral surfaces is likely to be an important process for removing organic compounds from the CO_2 as it moves from the storage reservoir to the aquifer. This would be particularly true for the heavier organic compounds, such as naphthalene, as demonstrated by the data in Figure 9a. The data in Figure 9a suggest that removal of benzene from CO_2 could be minimal; however, these columns are very short (10 cm) in comparison to the 1,000's of meters that the CO_2 would likely have to travel between the reservoir and the aquifer. The simple calculation illustrated here also does not account for advection and dispersion. In the model scenario of Fahrner et al. (2012), the pore velocity was 7 m/yr. As a result, neglecting these two processes would not likely significantly reduce the groundwater concentrations of the organic compounds in this assessment. In contrast, biodegradation in groundwater under aerobic conditions was expected to occur readily and would likely significantly reduce the concentrations of organic compounds within the aquifer over the course of one year (Aronson et al., 1999). Aronson et al. (1999) reviewed aerobic degradation rates for a number of organic compounds. The data they reviewed produced a median biodegradation rate for benzene of 0.096/day. This equates to a half-life of 7.2 days. Condensation of the organic compounds from the CO_2 as it decompresses from reservoir pressures to aquifer pressures would not be a factor in this case because their concentrations in the CO_2 were well below their saturation vapor pressures.

Although the quantities of light organic compounds extracted from the depleted oil reservoir rocks used in this study were very low, it is not likely that these samples are representative of the organic content of rocks that exist in situ. This is because these samples had been stored for years in a warehouse with no special precautions to preserve their VOC content. As a result, further work is necessary to estimate the quantities of organic compounds that could be mobilized from depleted oil reservoirs in the context of risk to an overlying aquifer.

2.5 CONCLUSIONS

Methods were developed to evaluate the mobilization and transport characteristics of organic compounds from geological carbon sequestration reservoir rocks and caprocks by $scCO_2$. Organic compounds studies using these methods were VOCs including BTEX, a PAH (naphthalene), and n-alkanes.

$ScCO_2$ was more effective for extracting VOCs and naphthalene from Gothic shale than CH_2Cl_2, while n-alkanes were much less extractable by $scCO_2$ than CH_2Cl_2. Dry $scCO_2$ extracted more toluene, but less naphthalene than water saturated $scCO_2$. Differences in the extractability of other organic compounds mobilized from Gothic shale by dry $scCO_2$ relative to water saturated $scCO_2$ were minimal.

Differences observed in the extractability of organic compounds from Fruitland coal by dry and water saturated $scCO_2$ were also small, but appeared to be correlated with the H-acceptor parameters of the organic compounds. Extraction of organic compounds by $scCO_2$ reached steady state by 96 h. Lighter compounds were more susceptible to mobilization by $scCO_2$ compared to heavier compounds. Normal alkanes with carbon numbers of 20 and higher were virtually unextractable by $scCO_2$.

When the $scCO_2$ with mobilized organics was released from the reactor and injected through sand columns, less than 60% of the lighter compounds (benzene, toluene) were retained in dry sand columns, while more than 90% of the heavier organic compounds were trapped in the dry sand column. In comparison, less than 20% of the organic compounds were trapped in wet sand columns, except naphthalene.

Based upon results determined for the reservoir rock, caprock, and coal samples studied here, no significant risks to aquifers from contamination by organic compounds were identified. Because it appears that the EOR reservoir samples were not preserved to prevent volatilization of organic compounds, further work will be necessary to fully evaluate risks from depleted oil reservoirs. A modeling approach is underway to address this issue.

3. TRANSPORT OF ORGANIC CONTAMINANTS MOBILIZED BY $_{SC}CO_2$ FROM COAL THROUGH A SANDSTONE

3.1 INTRODUCTION

Geologic carbon storage (GCS) is considered one of the primary options for long-term storage of large volumes of anthropogenic CO_2 to mitigate global warming (Bachu, 2000; White et al., 2003; Bachu and Adams, 2003). At the pressure and temperature conditions of GCS reservoirs, the stored CO_2 occurs as a supercritical phase. Supercritical CO_2 ($scCO_2$) is a strong solvent for organic compounds (Anitescu and Tavlarides, 2006; Kolak and Burruss, 2006), and is capable of extracting compounds from sedimentary rocks and other geological samples (Jaffé et al., 2000; Akinlua et al., 2008). Depleted oil reservoirs and coal formations are being considered as GCS reservoirs for CO_2 storage. During contact of $scCO_2$ with residual oil or coal in these reservoirs, toxic organic compounds will be extracted into the $scCO_2$ phase. As a result, concerns have been raised regarding the potential for groundwater contamination by toxic organic compounds mobilized from GCS sites (Xu et al., 2007; Kharaka et al., 2009). Although the integrity of the storage reservoir is one of the most important characteristics for GCS site selection, minor CO_2 leakage through faulty well casings, fractures and faults is possible. Mobilization of toxic organic compounds including BTEX and PAHs by $scCO_2$ has been reported in laboratory experiments for rock samples from depleted oil reservoirs, coal deposits (Zhong et al., 2014), and sandstones (Scherf et al., 2011). Groundwater monitoring results from GCS demonstration sites have shown increased concentrations of BTEX, PAHs, phenols, and other toxic compounds in groundwater after CO_2 injection (Scherf et al., 2011; Kharaka et al., 2011, 2010b, 2009). For example, dissolved organic compound concentrations were found to increase by more than 140 times in site groundwater after CO_2 injection (Kharaka et al., 2010b). Data are needed to assess the risks to groundwater contamination by toxic organic constituents mobilized by $scCO_2$ injection at GCS sites and subsequent transport to shallow drinking water aquifers via leakage pathways.

While the mobilization of organic contaminants by $scCO_2$ from GCS reservoir formations has been confirmed, and increased concentrations of these contaminants in groundwater at CO_2 injection sites have been reported, the retention and distribution of these compounds during transport is unknown. Many studies have reported on the transport of VOCs and PAHs through the vapor phase in the vadose zone. Both diffusion and advection may be important processes for VOC and PAH vapor plume spreading (Rivett et al., 2011). Phase partitioning of VOCs between the vapor phase and liquid phase is the dominant pathway for VOC contamination of groundwater from the unsaturated zone (Jang and Aral, 2007; Thomson et al., 1997). Sorption processes including absorption into water, soil organic matter, mineral-air interfaces, and mineral-water interfaces, retards the transport of organic compounds in the vapor phase (Goss, 2004). These principles, applicable to VOC and PAH vapor transport by air, may be different for transport of organic compounds by CO_2 as the gas moves through leakage pathways to the vadose zone. When CO_2 leaks from the storage reservoir, it will transform from a supercritical phase to a liquid phase and then a vapor phase as pressure and temperature are reduced. Interactions of organic compounds in the CO_2 gas with the aqueous phase and geologic materials could potentially be quite different than those in air. There are no theoretical or experimental studies at this time regarding the transport of organic compounds mobilized by CO_2 from a GCS reservoir to the shallow aquifer and ground surface.

In this study, $scCO_2$ containing mobilized organic compounds was released from a reactor and injected through rock cores to study the transport of the mobilized organic compounds. The mobility and phase distribution of the organic compounds were investigated as a function of temperature and pressure.

3.2 MATERIALS AND METHODS

3.2.1 Materials

Fruitland coal from the Pump Canyon Site, New Mexico, was selected as the source rock for organic mobilization (Zhong et al., 2013). This material was collected from a depth of 3,893 ft. The coal was crushed and sieved. Particles less than 1.0 mm were used in the experiments. The sandstone core was used as the porous medium in the transport experiments. The core sample was collected from a well drilled in Morgan County, Illinois, within the Lombard member of the Eau Claire formation at a depth of between 3,774 and 3,782 ft. Measured porosity of the rock was 12.5% and the permeability was 138 millidarcy (md) as determined by conventional plug analysis. The original sandstone cores received from the site had a diameter of 2.5 in. These cores were cored into 1.0-in. diameter rods. These smaller cores were then sliced perpendicularly to the axis into 1-in. length pieces. No organic carbon was detected in the rock samples prior to the transport experiments.

3.2.2 Methods

The experimental setup for the study is shown schematically in Figure 10. The setup includes two sections, one for the extraction of organic compounds by $scCO_2$ and the other for transport of the mobilized compounds through the rock cores. In the mobilization section, a Parr reactor (300 mL) with a heat jacket and temperature control system was used to extract the Fruitland coal with $scCO_2$. A coal sample (45 g) with a particle size of <1.0 mm was used for the extractions. A vial of 1.5 mL of DI water was placed in the reactor with the coal sample. Based on the water solubility in $scCO_2$ (Spycher et al., 2003), the $scCO_2$ was saturated with water at the test conditions of all the experiments. An ISCO syringe pump was used to charge and pressurize the reactor with CO_2. The pressure and temperature were adjusted to desired values and monitored over the course of the experiment. A needle valve was used to control the flow rate of CO_2 released from the reactor for the transport experiments, mimicking a $scCO_2$ leak from a GCS reservoir. The pressures and temperatures before and after gas release were used to calculate the CO_2 mass released from the reactor. The total pressure drop during the gas release was limited to less than 10% of the initial pressure to minimize any potential change in concentrations of the extracted organic compounds in the $scCO_2$.

A tri-axial core holder (Figure 10) placed inside an oven was used for the transport tests. Six 1-in. rock cores were stacked and wrapped with aluminum (Al) foil and placed within a rubber sleeve inside the core holder. The Al foil was used to prevent contact and sorption of organic compounds into the rubber sleeve. Before the gas transport test, the cores were wetted with DI water. DI water was injected into the core holder through the bottom end and water effluent was collected from the top end effluent line. Water was then allowed to drain from the cores and then air was passed through the cores to establish residual water saturation. The water saturation in the cores was determined gravimetrically.

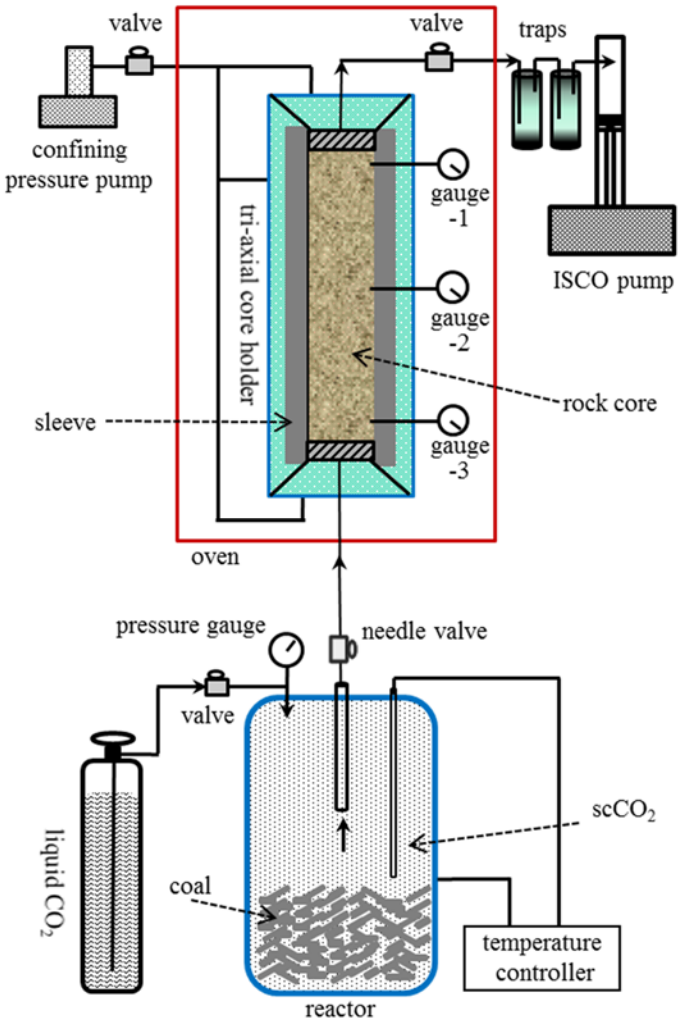

Figure 10: Schematic of experimental setup.

During the transport tests, the confining pressures were applied both around the rock cores and to the ends of the cores at a pressure of approximately 200 psi higher than the injection pressure. This higher confining pressure was used to ensure the gas flowed through rather than around the rock cores. The effluent pressures were set at 0, 500, and 1,000 psig (Table 6) to simulate leakage to different subsurface depths. For experiments with 0 psig effluent pressure, the effluent was directed through two CH_2Cl_2 traps assembled using glass vials, and then to the atmosphere. For the 500 and 1,000 psig effluent pressures, an ISCO pump was connected to the effluent. The pump was set at constant pressure mode to provide the desired pressure. Two 50-ml volume stainless steel vessels (ID = 2.54 cm) containing 30 ml CH_2Cl_2 were installed between the tri-axial core holder effluent and the ISCO pump to serve as traps for the organic compounds.

The core was set up vertically and gas flowed into the core from the bottom (Figure 10). At the completion of the gas flow experiment, the gas under pressure in the cores was released slowly and the confining pressure was relaxed. The core holder was then disassembled and each of the core pieces was extracted with CH_2Cl_2 for 48 h to remove the organic compounds for analysis. Preliminary tests demonstrated that extraction of the organic compounds from the core samples

was complete by 48 h. The influent line connecting the reactor to the core holder and the effluent line connecting the core holder to the CH_2Cl_2 traps were also flushed with CH_2Cl_2, which was then analyzed to determine if any organic compounds were retained within these lines.

Table 6: Summary of Experiments for Organic Compound Transport through Rock Core

Test Name	Effluent Pressure/Core Temperature	Source Rock; Pressure/Temperature For Extraction	Sampling Approach	Notes
CF-1	0 psig/20°C	Fruitland coal; 1,500 psig/95°C	Two CH_2Cl_2 traps for effluent (at 0 psig); extraction from segmented cores	Effluent CH_2Cl_2 traps were under ambient pressure and temperature
CF-2	500 psig/20°C	Fruitland coal; 1,500 psig/95°C	Two CH_2Cl_2 traps for effluent (500 psig); extraction from segmented cores	Effluent CH_2Cl_2 traps were under 500 psig pressure and temperature
CF-3	1,000 psig/20°C	Fruitland coal; 1,500 psig/95°C	Two CH_2Cl_2 traps for effluent (1,000 psig); extraction from segmented cores	Effluent CH_2Cl_2 traps were under 1,000 psi pressure and temperature
CF-4	1,000 psig/50°C	Fruitland coal; 1,500 psig/95°C	Two CH_2Cl_2 traps for effluent (1,000 psig); extraction from segmented cores	Effluent CH_2Cl_2 traps were under 1,000 psig pressure and temperature

The organic compounds in the CH_2Cl_2 traps were identified and quantified using an Agilent Technologies 5975C GC-MS system. An Agilent capillary column (0.25 mm × 30 m × 0.25 µm) was used to separate the organic compounds. Commercial standards of BTEX and naphthalene were used for calibration. The temperature of the GC column was initially set at 32°C, held for 2 minutes, ramped up at 5°C/minute to 280°C, and then held at this temperature for 5 minutes. In this study only BTEX compounds and naphthalene were analyzed. The properties including the Henry's law constant, K_H, for these compounds are summarized in Table 7.

Table 7: Properties of Analyzed Compounds

Organic Compounds	Formula	MW	K_H[a] (Pa-m^3/mol.)	K_H[a] Dimensionless	MCL (mg/L)
Benzene	C_6H_6	78.11	531[b]	0.218	0.005
Toluene	C_7H_8	92.14	679[c]	0.279	1.0
Ethylbenzene	C_8H_{10}	106.17	669[c]	0.275	0.7
m&*p*-Xylene	C_8H_{10}	106.17	709[c,d]	0.291[d]	10 (total xylenes)
o-Xylene	C_8H_{10}	106.17	561[b]	0.231	10 (total xylenes)
Naphthalene	$C_{10}H_8$	128.17	36[c]	0.015	NA (possible human carcinogen)

(a) At 20°C and ambient pressure
(b) Mackay and Shiu (1981)
(c) Montgomery and Welkom (1990)
(d) For *m*-Xylene

3.2.3 Modeling

Reactive transport modeling was used to analyze the experimental results with respect to the mechanisms that governed the deposition of the organic compounds within the column during the flow-through experiments. The Subsurface Transport Over Multiple Phases (STOMP) simulator (White and Oostrom, 2006), developed by the Pacific Northwest National Laboratory to predict thermal and hydrological flow and reactive transport in variably saturated subsurface environments, was used for this purpose. It is a multiphase, multi-component reservoir code used extensively in environmental and gas/CO_2 modeling applications. STOMP solves nonlinear partial differential equations for the conservation equations, with reactive transport occurring over mobile phases. The coupled hydrologic transport and mixed geochemical reaction systems are solved using an operator splitting approach with no iteration between the transport and reaction systems. The chemistry module ECKEChem (Equilibrium-Conservation-Kinetic-Equation Chemistry) solves mass balance equations, mass action equations, and kinetic equations simultaneously using the Newton-Raphson approach (White and McGrail, 2005). The simulator has several different operational modes, i.e., different source code depending on the solved governing equations (e.g., water mass, air mass, dissolved-oil mass, oil mass, salt mass, thermal energy), from which users can choose.

For this application, the STOMP-WNE (water, N-component, energy) operational mode was used. STOMP-WNE simulates nonisothermal, multiphase flow of water and gas mixtures with an arbitrary number of components. Gas mixture properties are calculated using a Peng-Robinson cubic equation of state (Peng and Robinson, 1976), and the solubility of the gas components in water are calculated using Henry's Law.

3.3 RESULTS

3.3.1 Mass Transport of Organic Compounds through the Column

The mass percentages of organic compounds that were transported through the columns relative to those released from the extraction vessel are shown in Table 8. These results indicate that most (81–98%) of the BTEX compounds were readily transported through the columns without

interaction. The behavior of naphthalene was very different than that of the BTEX compounds with only 3.5–4.9% moving through the columns. For the columns conducted at 20°C (CF-1, CF-2, and CF-3), a clear trend is observed for the BTEX compounds with increasing column effluent pressure. As the effluent pressure increased from 0 psig (CF-1) to 1,000 psig (CF-3), the percentage of BTEX compounds that moved through the columns decreased. This behavioral trend was generally consistent for each of the BTEX compounds. The increase in temperature from 20°C (CF-3) to 50°C (CF-4) at a column effluent pressure of 1,000 psig significantly increased the transport of the BTEX compounds within the column. The influence of pressure and temperature on transport of naphthalene through the columns was generally consistent with the trends observed for the BTEX compounds.

Table 8: Mass percent of Organic Compounds Transported through the Column

Compound	CF-1	CF-2	CF-3	CF-4
Benzene	95.6	90.5	90.0	94.5
Toluene	97.8	94.6	91.9	98.2
Ethylbenzene	93.6	87.2	82.8	93.9
m&*p*-Xylene	97.0	87.4	86.2	97.3
o-Xylene	96.7	84.3	80.8	96.8
Naphthalene	4.9	3.5	3.6	4.6

The mass percentage of BTEX compounds retained in the columns as a function of pressure is shown in Figure 11. The results clearly illustrate that as pressure increases, retention of the BTEX compounds within the columns increases. In addition, retention at elevated pressure generally increases with increasing molecular weight of the BTEX compounds.

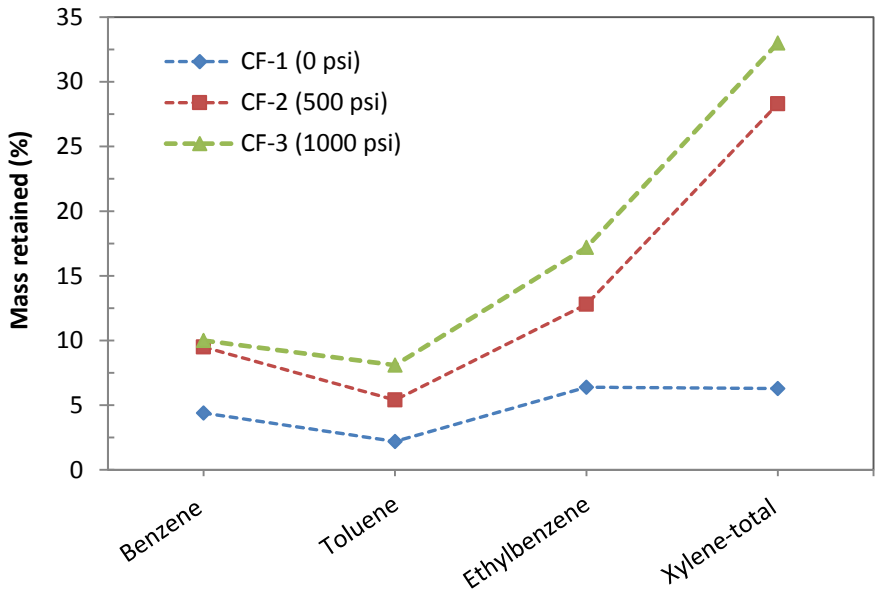

Figure 11: Mass percent of organic compounds retained within the columns as a function of pressure (at 20°C).

The mass percentage of organic compounds retained in the columns as a function of temperature is shown in Figure 12. These results show that as temperature decreases, retention of the BTEX compounds within the columns increases. In addition, retention at lower temperature generally increases with increasing molecular weight of the BTEX compounds.

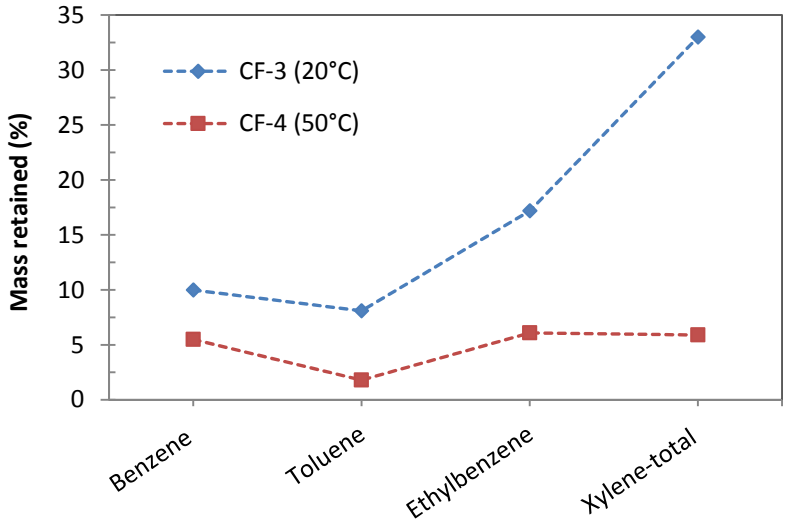

Figure 12: Mass percent of organic compounds retained within the columns as a function of temperature at 1,000 psig.

3.3.2 Distribution of Organic Compounds within the Column

The concentrations of organic compounds retained in the cores obtained for Test CF-1 are shown in Figure 13 for the BTEX compounds and in Figure 14 for naphthalene. The concentrations for all compounds exhibited decreases from the first core to the last core. For benzene and toluene, the decrease in concentrations was relatively gradual, with concentrations in the last core being greater than 65% of that in the first core. For ethylbenzene and xylene, the concentrations decreased more rapidly, with the last core showing concentrations that were less than 50% of that in the first core. For naphthalene, the decrease in concentrations along the column was much more dramatic, decreasing to zero in the last core.

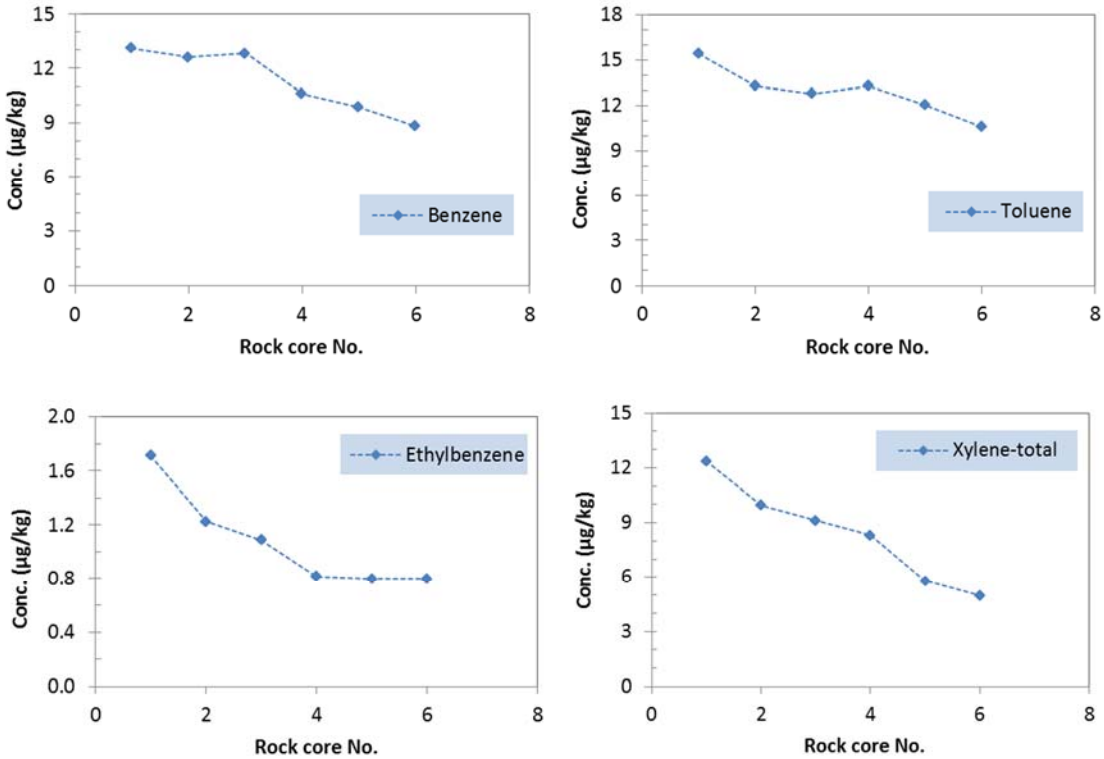

Figure 13: BTEX compound concentration distribution in rock cores from Test CF-1 (20°C and ambient pressure). Rock cores were numbered No. 1 through No. 6 from the inflow end of the column.

The concentration distribution patterns in the columns were similar for all four tests. For Tests CF-1 (20°C and ambient pressure) and CF-3 (20°C and 1,000 psig), the mass percentages of the organic compounds retained by each core are displayed in Figure 15. Benzene and toluene displayed the most gradual decreases from the first core to the last core, followed by ethylbenzene and xylene. Naphthalene exhibited the most sizable decreases in concentration along the length of the column.

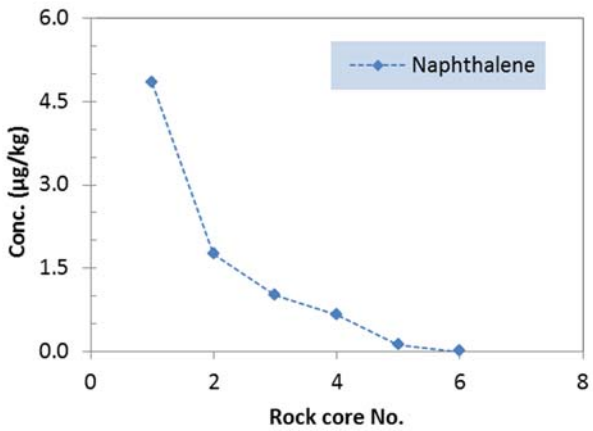

Figure 14: Naphthalene concentration distribution in rock cores in Test CF-1 (20°C and ambient pressure).

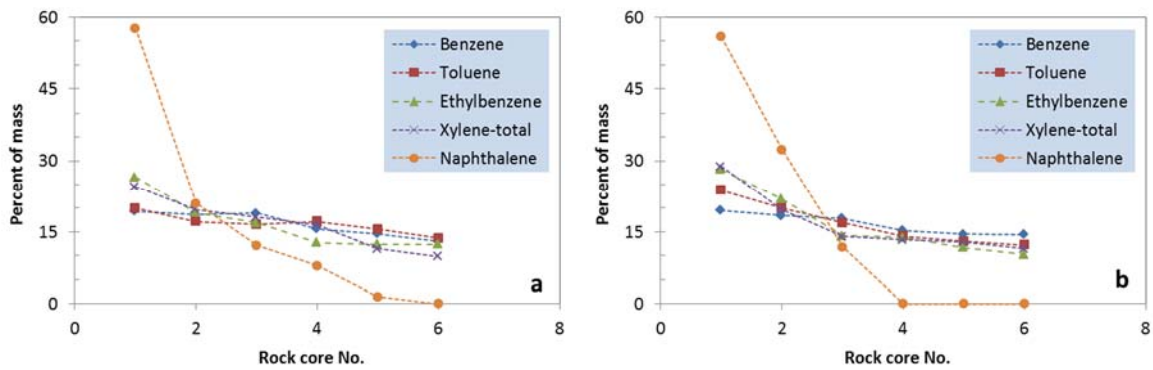

Figure 15: Percent of retained organic compound mass in each core in the total retained mass for tests CF-1, 20°C and ambient pressure (a), and CF-3, 20°C and 1,000 psig (b).

In previous work, it was found that adsorption of BTEX compounds and naphthalene to the surfaces of dry quartz sand was relatively high, but was reduced significantly when the sand was coated with water (Zhong et al., 2014). A similar observation was also reported by Cabbar and Bostanci (2001). In this work, the sandstone core did not contain any detectable quantity of organic matter and was coated with water prior to the experiment. As a result, it was hypothesized that dissolution from the vapor phase into the aqueous phase was the primary mechanism responsible for retention of organic compounds in the columns. To test this hypothesis, reactive transport modeling of the organic compounds in column CF-1 was conducted.

Figure 16 is a plot of the concentrations of organic contaminants determined in the cores of the column CF-1 (20°C and ambient pressure) by assuming that all the organic compounds retained within the column had dissolved into the water phase (experimental results are indicated with symbols). The modeling results are indicated with solid lines. The modeling was conducted using the dimensionless Henry's Law constants for 20°C (Table 8). For the BTEX compounds, the modeling results indicated that the concentrations should be constant throughout the length of the column. This was because the quantity of gas injected through the column was sufficient,

such that the water should have reached equilibrium with the vapor phase concentrations throughout the column during the course of the experiment. For benzene, the experimental results and the model results were very similar, suggesting the equilibrium between the vapor phase concentration and the water phase did in fact occur or came very close. For toluene, xylene (total), and ethylbenzene, the model results approximated the experimental results reasonably well, but deviate more significantly than was the case for benzene. These more significant differences between the experimental and modeling results may be due to uncertainties associated with the Henry's Law constants that were used. The cause of the decrease in concentration of the BTEX compounds along the length of the column has not been determined. Adsorption of BTEX compounds to inorganic materials that contain low concentrations of organic matter is weak (Joo et al., 2012; Piwoni and Banerjee, 1989). For example, partition coefficients for benzene on aquifer materials with low organic matter content measured in one study ranged from 0.026 to 0.038 L/kg (Piwoni and Banerjee, 1989). When adsorption was included in the modeling, the concentrations of BTEX compounds would increase, but would remain constant along the length of the column. Based on these results, it was concluded that partitioning into the water phase was the predominant mechanism controlling retention of BTEX compounds in the column experiments.

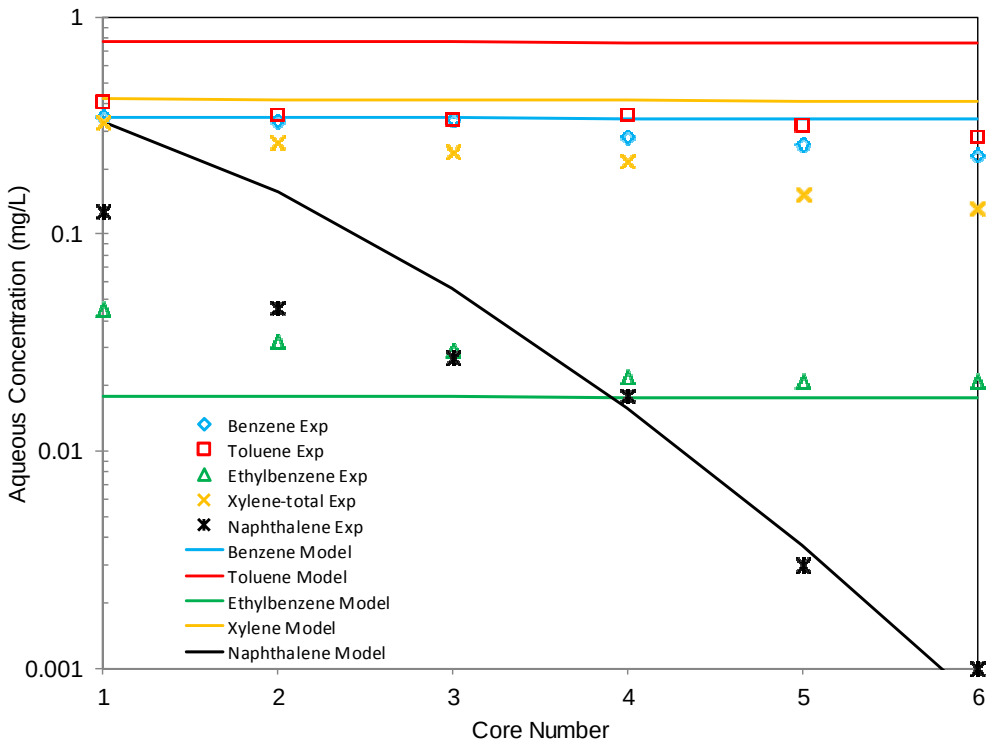

Figure 16: Concentration of organic contaminants of pore water in the rock cores for Test CF-1 (20°C and ambient pressure).

The results for naphthalene (Figure 16) show a much greater reduction in concentration along the length of the column than occurred for the BTEX compounds. Initial modeling results for

naphthalene that considered only partitioning between the vapor phase and the water phase resulted in a constant concentration throughout the column (not shown) as was the case for the BTEX compounds. This result was clearly inconsistent with the experimental results. It was determined that two additional factors had to be considered in order to get the model curve shown in Figure 16. The most important factor was that most (93.3%) of the naphthalene had precipitated within the influent line before entering the column. Accounting for this greatly reduced the concentration of naphthalene that was calculated to occur within the column and was more consistent with the measured results; however, the model results indicated that the concentrations would still be constant throughout the column. To get the down-trending curve shown in Figure 16, adsorption onto the solid matrix also had to be included in the model. The model result shown in Figure 16 was obtained by accounting for the reduced influent concentration and by assuming an adsorption coefficient for the rock core material of 0.0013 L/kg. Accounting for these processes in the model produced a result that was in reasonably good agreement with the experimental results.

Because Henry's Law constants are not applicable at high pressures, transport modeling was performed only with the data from column CF-1. Although partitioning coefficient data for $scCO_2$ and water was available for some compounds at high pressure (Burant et al., 2013), data was not available at the conditions used in these experiments.

3.4 DISCUSSION

The results presented here indicate that for leakage scenarios in which $scCO_2$ containing organic compounds dissolved from organic rich carbon sequestrations reservoirs such as coal deposits and depleted oil reservoirs, the transport of the organic compounds will be significantly retarded by dissolution into the aqueous phase present in geologic materials through which the CO_2 passes. In this scenario, heavier organic compounds such as PAHs are significantly less mobile than lighter compounds such as BTEX. Several factors contribute to this outcome. BTEX have significantly larger Henry's Law constants and water-$scCO_2$ partition coefficients than PAHs, indicating a preference for the gas or $scCO_2$ phase over water relative to PAHs. In addition, adsorption onto wet mineral surfaces is greater for PAHs than BTEX compounds due to its greater hydrophobicity (Schwarzenbach and Westall, 1981; Schwarzenbach et al., 2003). Although not addressed in this study, subsurface materials with significant organic material could potentially adsorb significant amounts of organic compounds mobilized by $scCO_2$ (Schwarzenbach et al., 2003).

Deep geologic reservoirs that are planned for carbon storage have elevated pressure and temperature. The results presented here indicate that these factors will have a significant effect on the transport of mobilized organic compounds in the subsurface. Increased pressures were found to increase partitioning of mobilized organic compounds from the vapor phase to the aqueous phase, while increased temperature had the opposite effect, with higher temperatures favoring retention of mobilized organic compounds in the vapor phase.

4. DETERMINATION OF ORGANIC PARTITIONING COEFFICIENTS IN WATER-SUPERCRITICAL CO_2 SYSTEMS BY SIMULTANEOUS IN SITU UV AND NEAR-INFRARED SPECTROSCOPIES

4.1 INTRODUCTION

As energy demands increase with expanding global population and prosperity, so do emissions of CO_2 into the atmosphere. Several methods including energy conservation, use of alternative energy sources, and storage of produced greenhouse gasses have been suggested to reduce emissions of greenhouse gasses. It is generally accepted that some combination of these methods may be employed to control the growing atmospheric CO_2 levels (Mathieu, 2006). One promising method, which is gaining public acceptance, is geologic carbon sequestration (GCS) (Bachu and Adams, 2003; Benson and Surles, 2006; Benson and Cole, 2008). GCS entails storage of CO_2 in various geologic features such as deep saline aquifers, depleted oil and natural gas reservoirs and un-mineable coal seams (Bachu and Adams, 2003). Use of CO_2 in EOR applications is well documented (Bondor, 1992; Blunt et al., 1993; Mathieu, 2006); however, much of the utilized CO_2 is recovered. Many of the same reservoirs where EOR is practiced could be used for storage of CO_2 collected from power plants (Bachu and Adams, 2003; Godec et al., 2011).

At typical GCS storage depths, CO_2 will be held at pressures and temperatures well above the critical point (73.8 bar, 31.1°C) (Kordinkowski et al., 1996). In the supercritical phase, CO_2 is an effective solvent for non-polar organic compounds and other contaminants, a trait that has been well documented and employed in industry for many years (McHugh and Krukonis, 1986; Morgenstern et al., 1996; Karasek et al., 2002; Anitescu and Tavlarides, 2006). This poses unique contamination risks for a $scCO_2$ storage program where residual organic matter is present, such as in depleted oil reservoirs. Many of the compounds found in crude oil are toxic or carcinogenic, including benzene and various benzene derivatives such as BTEX, as well as PAHs. In the event of a leak, stored CO_2 could potentially escape into overlying groundwater aquifers (Hawkes et al., 2005; Mathieu, 2006), carrying with it organics extracted from the storage reservoir (Zheng et al., 2013).

In an effort to better assess the risks of contaminant mobilization, it is necessary to develop a fundamental understanding of pertinent organic contaminant behavior at conditions (temperature, pressure and ionic strength of brine solutions) similar to those found in possible storage sites (Burant et al., 2013). By understanding how organic contaminants behave in binary systems of $scCO_2$ and water/brine, predictions may be made regarding contamination risks associated with leak scenarios. The distribution of an organic contaminant in each of these two phases is described by the partitioning coefficient (K). Timko et al. (2004) provides a summary of available data for organic contaminant partitioning coefficients in water-CO_2 systems. There are several limitations in the available data set (Timko et al., 2004). First, partitioning coefficients have been measured for a relatively small number of compounds. Notably absent are ethyl benzene and the xylene isomers, as well as any representative long-chain saturated hydrocarbons, such as dodecane. Additionally, the scope of conditions investigated show considerable variation, resulting in gaps in the data. Moreover, the impact of ionic strength effects on K values does not appear to have been investigated. Finally, the available data for benzene exhibits considerable uncertainty (Yeo and Akgerman, 1990; Ghonasgi et al., 1991). Some of this uncertainty may be due to the use of ex-situ measurement techniques in one or both phases. For

relatively non-volatile compounds, errors produced due to escape of organic vapors during sampling may be small; but for highly volatile compounds such as benzene, such errors may be significant.

In this work, a new method was developed for measuring organic partition coefficients in $scCO_2$-water systems using in-situ spectroscopic measurements of both phases. Concentrations of organics in the CO_2-rich phase were measured in a custom reactor by near-infrared spectroscopy (NIRS), while simultaneous aqueous-phase measurements were performed by circulating the fluid past an in-line ultraviolet (UV) detector. The unique apparatus employed a high-pressure titration capability that allowed precise additions of a pollutant of interest to the pressurized reactor (Fonseca et al., 2011). This arrangement allowed for real-time observation of the contaminant's partitioning behavior. Additionally, due to the high level of repeatability of the injection volume, reliable mass-balance checks may be performed to validate measured concentrations and ensure that a third, non-aqueous phase has not formed. The system was initially applied to quantify the partitioning behavior of benzene due to inconsistencies in previous measurements and benzene's low EPA drinking water standards and associated health risks (da Costa and da Costa, 2002; Huff, 2007; Wilbur et al., 2008; Galbraith et al., 2010). Some scoping measurements were also conducted with toluene that demonstrate some of the limitations of this approach.

4.2 METHODS AND MATERIALS

4.2.1 Theory

Partitioning coefficient at a given temperature and pressure, $K_{t,p}$, is defined as the ratio of mole fraction in the CO_2 phase (y_i) to that in the water phase (x_i) (Yeo and Akgerman, 1990; Brudi et al., 1996). These mole fractions are determined using the concentrations of organic measured in each phase as well as densities as found in IUPAC-tables. When expressed as a function of measured concentrations, $K_{t,p}$ may be found using:

$$K_{t,p} = \frac{C_{CO_2} * (C_{H_2O} + \frac{D_{H_2O}}{MW_{H_2O}})}{C_{H_2O} * (C_{CO_2} + \frac{D_{CO_2}}{MW_{CO_2}})} \quad (1)$$

where C_{CO2} and C_{H2O} represent organic concentration in the CO_2 and H_2O phases respectively, D_{CO2} and D_{H2O} represent densities of the solvent (CO_2 or water) at the experimental temperature and pressure, and MW_{CO2} and MW_{H2O} are the molecular weights of the solvents, CO_2, and water, respectively.

Figure 17 shows density trends for CO_2 plotted as a function of pressure for temperatures used in this study. At low pressures which corresponded to the gas phase realm, there was limited change in density as pressure was increased. As the critical point was approached, density increased rapidly with pressure increase until the conditions were well into the supercritical range, at which point small changes in density were observed as pressure was increased. Additionally, qualitative comparison of trends in density between the plotted temperatures indicated that the dramatic increase in density near the critical point was less pronounced in the higher temperature data (T=65ºC) than in the lower temperature data. At high temperatures, it

appears the density-pressure relationship approaches linearity while at lower temperatures it does not. Being that the dependence of solubility on supercritical fluid density has been established previously (Chrastil, 1982), it follows that density should be one of the major factors which influence partitioning of compounds of interest between water and $scCO_2$.

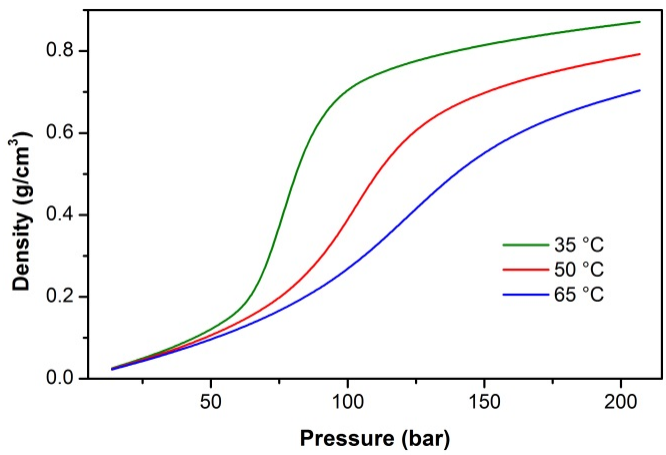

Figure 17: CO_2 density as a function of pressure for the temperatures used in this study. Densities were calculated using the software program EOS-SCx (Tsutomu Ohmori, http://hp.vector.co.jp/authors/VA030090/).

4.2.2 Apparatus

Measurement of partitioning coefficients was carried out using the apparatus shown in Figure 18. Samples were prepared in the high pressure cell, machined in grade 3 titanium by Parr Instrument Company (Moline, Illinois). The reactor was fitted with a pair of 0.5-in. thick, 1-in. diameter colorless quartz windows through which to measure spectra of the supercritical phase as well as cartridge heaters and threaded ports for both the titration system and the aqueous sample loop. A third 0.5-in. thick quartz window was installed flush with the floor of the reactor so that effective stirring of the aqueous phase could be confirmed during the course of the experiment. A rupture disk was also fitted to the head of the reactor rated to 193 bar for safety. A 5-point J-type thermocouple contained in titanium sleeve as well as a pressure transducer were installed to closely monitor the conditions inside the reactor, and this setup was interfaced with a 24-bit USB data acquisition board (Measurement Computing model 2416 4AO) for data collection. Pressure, temperature, and UV absorbance data were acquired, displayed and logged by custom software (Embarcadero C++ builder Professional). The reactor was mounted in a custom designed magnetic stirring apparatus attached to the base of the spectrometer. The stirrer assembly also provided a scaffolding on which to mount the necessary valves and tubing for both the titration loop and the UV measurement loop. Constant stirring of the water phase was achieved using a Pyrex coated magnetic stir bar to minimize possible sorption of benzene or other organics measured. Pressurized CO_2 was provided to the system by an ISCO model 260D syringe pump running in constant pressure mode.

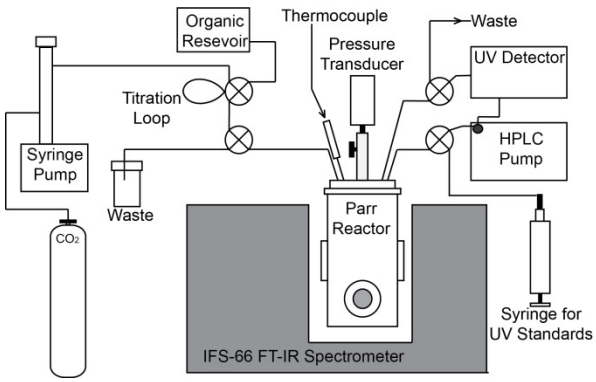

Figure 18: Schematic of the high-pressure titration system with dual spectroscopic detectors.

4.2.3 Spectral Measurements

NIR spectra of the CO_2 phase were recorded with a Bruker IFS66 spectrometer equipped with a tungsten light source and a silicon diode detector. Sampling was carried out through the reactors quartz windows with a path length of 5.639 cm. Spectra were recorded from 4,000–14,000 cm^{-1} with a 2 cm^{-1} resolution. The interferometer was scanned at a rate of 1.00 cm/s and 128 scans were co-added for each spectrum collected. For each experiment the reactor was heated to the desired temperature, filled with CO_2 to the necessary pressure at which point a background was collected to be used in obtaining absorbance spectra of the prepared samples. Once the background was obtained, the desired experimentation (CO_2 phase calibration or K value measurement) was carried out via the titration loop. For all NIR samples a linear baseline correction was applied by subtraction of the line fit through average absorbances between 6,255–6,282 cm^{-1} and 5,736–5,752 cm^{-1}.

Water phase measurement was performed using sample loop constructed from 0.02-in. ID stainless steel tubing with Rheodyne valves plumbed to isolate the loop from the reactor for calibration purposes. The majority of this loop was jacketed with Tygon tubing and its temperature controlled via heated water bath. Liquid from near the floor of the reactor was pumped through the UV sample loop by a Gilson high-performance liquid chromatography (HPLC) pump, through a fixed wavelength Gilson-151 UV Visible detector (path length 0.5 cm) fitted with a high pressure cell and returned to the water phase in the reactor. All tubing in the apparatus downstream from the sample loop or directly in contact with either phase of the system was of stainless steel construction to further minimize sorption of organic material.

4.2.4 Calibration

To calibrate the volume of the PEEK sample loop, the reactor was first filled with a known volume of benzene and pressurized with $scCO_2$. Spectra were collected of the known-volume sample, and subsequently several injections of benzene were made using the titration loop. Benzene peak intensity of the titration samples was compared to that of the sample measured with a measured volume of benzene. By comparing the peak intensity at known concentration to those collected after injections from the loop, the loop volume was determined.

Separate calibrations were prepared for each of the two detectors. In the CO_2 phase, a calibration curve was prepared by first filling the reactor to the desired pressure and allowing temperature

equilibrium to be reached so that blank spectra may be collected. Once equilibrium was reached, aliquots of the organic of interest were titrated into the reactor by way of the loop system. These injections were repeated until the desired amount of organic had been injected, at which point spectra were collected. This process was repeated until two to four calibration points had been collected. Initial measurements showed small shifts in calibration slope between organics measured in wet and dry CO_2, on the order of a 9.8% reduction in slope. To ensure consistency between calibration conditions and conditions under which the samples were collected during partitioning coefficient measurement, 0.2 ml water was placed inside the reactor to saturate the CO_2 phase (Spycher et al., 2003). Spectra were treated with custom MATLAB scripts to correct for drifting baseline slope and extract integrated peak areas to generate calibration curves. The UV detector was calibrated for water phase measurements in each experiment using a single point calibration. A known volume of the organic of interest was injected into a measured volume of water and mixed thoroughly in a glass vial, minimizing headspace to prevent loss of organic compounds to the vapor phase. This standard then flowed through the detection loop while isolated from the reactor, after which the sample loop was flushed with water and moved in-line with the reactor so that water phase concentrations could be monitored and recorded for the duration of the experiment.

4.2.5 Determination of Reactor Volume

Due to the mounting of various dip tubes, injection lines and fittings to the reactor head which protruded into the interior, experimental determination of the internal volume of the reactor was required. This was achieved by observation of signal strength change before and after displacement of a known fraction of the reactors internal volume. Once the volume of the injection loop had been calibrated, known volumes of organic compounds were delivered into the reactor at 96.53 bar and 50ºC with and without reactor volume displaced. A custom insert was machined from aluminum to displace 49.56 ml of the reactor volume. Spaces were cut in the insert to allow the titration and circulation dip tubes to be left in place, and to allow for uninhibited stirring and spectral measurement through the CO_2 phase. By comparing intensity of the benzene signal for injections of the same volume made into the reactor with and without the insert in place, total reactor volume was determined using the relationship:

$$V_r = \frac{V_i}{1-\frac{A_1}{A_2}} \tag{2}$$

which is derived from Beer's Law where V_r is the volume of the reactor, V_i is the volume displaced by the insert, and A_1 and A_2 are the observed NIR absorbance collected in the reactor without and with the insert in place, respectively.

4.2.6 Partition Coefficient Measurements

The following protocol was used to measure partition coefficients. The desired temperature of the reactor was controlled with a thermostat; and once the temperature of the vessel had stabilized, it was filled with a weighed volume of DI water, re-sealed, and pressurized again to desired conditions. After equilibrating, the UV sample loop pump was started and water was circulated through the loop at a rate of 1 ml/min for the remainder of the experiment. Background spectra were collected in both the aqueous and CO_2 phases and the organic compound of interest was injected into the titration loop. Spectral measurements were collected

in both phases after injection, continuously in the UV and typically at 5-min intervals in the NIR, until the benzene absorbance had leveled off, which the authors interpreted as indicative of equilibrium. Measurement in both phases was used to ensure that a second phase was not present, and to ensure a mass-balance based confirmation of the measured K value. For benzene experiments, injections were made that established a starting benzene concentration in the water phase of approximately 7.5×10^{-3} M or 6 mg/L.

4.3 RESULTS

4.3.1 Benzene Spectra in Water and $scCO_2$

Spectra of benzene in both the water phase and CO_2 phase are shown in Figure 19. Water phase measurements are shown at ambient temperature and pressure (~22°C and approximately 1 bar), while CO_2 phase spectra are shown at 50°C and 96.53 bar. The NIR spectra of water/CO_2/ benzene shown display five distinct features. Peaks at approximately 7,200 and 5,300 cm^{-1} can be assigned to water (Takebyashi et al., 2011), specifically the $\nu_1+\nu_3$ and $\nu_2+\nu_3$ combinations, respectively, where ν_1 and ν_3 are the symmetric and anti-symmetric stretching modes and ν_2 is the bending mode for water. Peaks centered around approximately 6,250 cm^{-1} as well as the sharp peak found at approximately 6,970 cm^{-1} are indicative of CO_2 (Takebyashi et al., 2011). The grouping centered around 6,250 cm^{-1} is a tetrad partly obstructed by the benzene peak (approximately 6,000 cm^{-1}) and is due to the Fermi resonance of $3\nu_1+ \nu_3$, $2\nu_1+2\nu_2^0+ \nu_3$, $\nu_1+4\nu_2^0+ \nu_3$ and $6\nu_2^0+ \nu_3$ where ν_1 is the symmetric stretch of CO_2 and ν_2 is the CO_2 bending mode. C-H overtone stretching absorbance due to the presence of benzene is observed at approximately 6,000 cm^{-1} (Workman and Weyer, 2007). UV spectra of benzene show a local maxima at 254 nm, which was used for measurement in the water phase sample loop to maximize detection. This maxima is contained in a broad vibronic band attributed to the $A^1B_{2u} \leftarrow X^1A_{1g}$ electronic transition (Kometani et al., 2004).

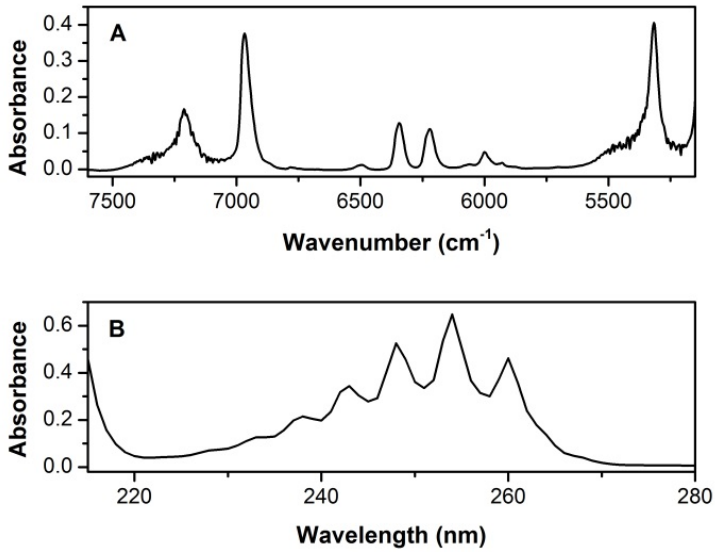

Figure 19: Benzene spectra: (A) near-infrared spectrum of a 0.0046 M solution of benzene in the CO_2-rich phase (50°C and approximately 97 bar), and (B) UV spectrum of a 0.0054 M aqueous solution at ambient conditions (22°C and approximately 1 bar).

4.3.2 Calibrations in Water and $scCO_2$

Figure 20 shows typical calibration spectra for benzene in both the CO_2 (NIR) and water (UV)-rich phases. In spectra collected for organics of interest in both the CO_2 and water phases, absorbance appears to vary linearly with the concentration of organic compound. Benzene concentrations were calculated as functions of integrated absorbance of the C-H overtone stretching band from 5,970 cm^{-1} to 6,020 cm^{-1}. The calibration prepared from these integrated spectra is shown in Figure 19, with an R^2 value of 0.997. Spectra recorded in the water phase were collected at a wavelength of 254 nm. To confirm absorbance linearity of benzene spectra at concentrations typical of these measurements, the calibration shown above was collected in DI water with an Agilent 8453 diode array spectrometer in quartz cuvette at ambient conditions.

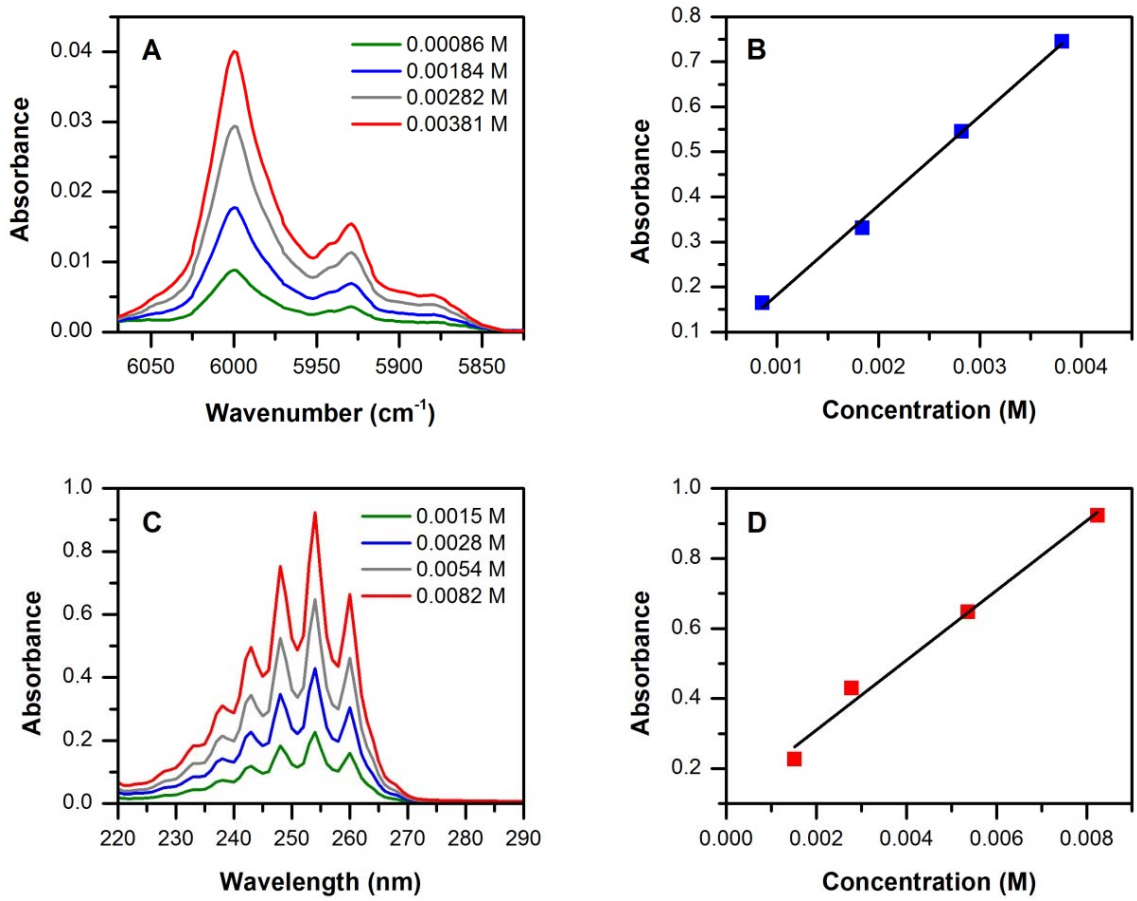

Figure 20: Representative benzene calibration data: (A) near-infrared spectra of benzene in the CO_2 phase, (B) plot of integrated near-infrared absorbance versus concentration, (C) UV spectra of benzene in water, and (D) plot of UV absorbance at 254 nm versus concentration.

4.3.3 In Situ Observation of Partitioning Behavior

Figure 21 shows typical concentration trends observed in partitioning experiments, with time displayed as minutes from injection of benzene. In the first 15 to 20 min after injection, a rapid loading of the water phase is observed as the benzene is injected into the aqueous phase, mixes, and dissolves. This is followed by transport into the CO_2 phase, observed as a decline in the water phase concentration over approximately 1 h. In the remaining time, there was a gradual decrease in aqueous phase concentration as equilibrium was established. Observation of change in absorbance in the water phase was used to determine whether equilibrium was yet established. Observation of the unchanged UV absorbance slope over times greater than 10 min was interpreted as an establishment of equilibrium. Typical time to equilibrium is approximately 2.5 h. In some cases, dramatic increases in absorbance of the water phase were observed. These were attributed to the formation of bubbles, probably in the pump head, which became lodged in the sample chamber of the UV detector. In these cases, the experiment was ended and repeated due to the lack of usable water concentration data.

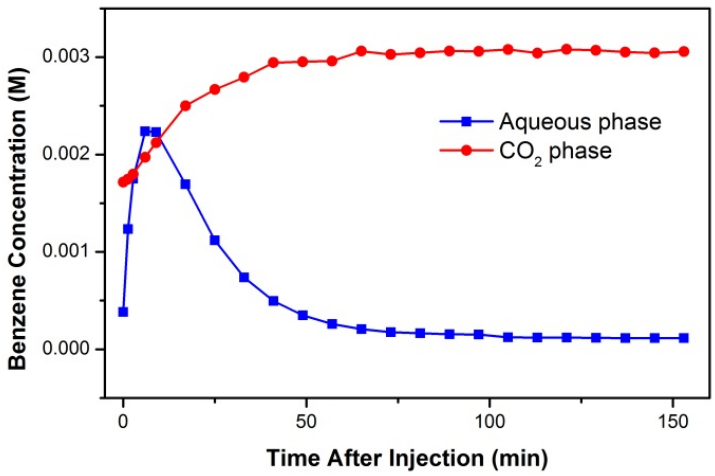

Figure 21: Concentrations of benzene in the aqueous and CO_2 phases after injecting benzene into the reactor.

Table 9 shows benzene partitioning coefficient values across a range of temperatures and pressures as measured in this study, as well as those values found experimentally via other methods (Ghonasgi et al., 1991; Yeo and Akgerman, 1990). Figure 22 shows experimental K values plotted by pressure. For all temperatures, there were relatively small increases in the partitioning coefficient at low pressures, which were representative of the CO_2 present in the gas phase. Additionally, at low pressure values below the critical pressure (P_c), the K values observed for all temperatures are relatively similar. Once the critical pressure is approached, K begins to increase more rapidly as the solvating power of the CO_2 phase increases and the spread between data points with similar pressures at the three temperatures become dissimilar. At or just above the critical pressure, there is a shift and K values increase dramatically with increasing pressure. This correlation of solvating power to supercritical fluid density agrees with other documented work on solubility behavior in supercritical fluid systems (Chrastil, 1982). In both the 35°C and 50°C data sets, a maximum is observed slightly above the critical pressure. As pressure continues to increase, K value decreases. This decrease may be explained by a dilution type effect. A comparison of benzene concentrations observed in the aqueous phase as a function of CO_2 phase density illustrates this. Figure 23 shows water phase benzene concentration plotted as a function of the density of the CO_2 phase. Initially, there was rapid decrease in water phase concentration consistent with previous observation that solvating abilities increase with increasing density of the supercritical phase. However, as density passes approximately 0.3 g/cm^3 water phase concentrations becomes relatively unchanged despite increasing density. While density of the CO_2 phase continues to increase, the solvation of benzene does not increase at the same rate, thus, the mole fraction of benzene in CO_2 is driven down while the water phase mole fraction which is unaffected by pressure remains relatively constant causing depreciation of the K values (Equation 1). This maximum is observed at the data point corresponding to 96.53 bar. In contrast, the 65°C data set exhibits a steady increase as the critical pressure is approached and subsequently passed. Comparing trends in CO_2 density (Figure 17) to the data sets shown below (Figure 22), the drastic shift in slope of the K value trend corresponded to the rapid increase in CO_2 density for 35°C and 50°C; however, this increase in density was less marked at 65°C. As such, it seems likely that a similar depreciation in K value for 65°C

experiments may be observed; however, this would occur at pressures much higher than those included in the conditions of this work.

Table 9: Benzene Partitioning Coefficients Determined in this Study and from Ghonasgi et al. (1991) and Yeo and Akerman (1990)

Pressure (bar)	35°C	40°C	50°C	65°C
24.68	30.65	—	31.7	47.5
53.70	34.7	—	43.3	45.8
67.13	48.6	—	51.5	48.3
77.75	—	856.7[(a)]	—	—
80.55	64.4	—	75.7	67.8
87.88	—	1626.3[(a)]	—	—
93.98	315.8	1957.8[(b)]	176.7, 981.82[(b)]	79.5
98.01	—	2756[(a)]	—	—
107.41	—	3809.6[(b)]	1648.1[(b)]	—
120.83	180.8	3726.4[(b)]	130, 1252.1[(b)]	—
134.45	—	3645.9[(b)]	2324.6[(b)]	173.8
147.78	154.4	4102.3[(b)]	1654.2[(b)]	—
161.15	—	4941.2[(b)]	2553.1[(b)]	253.1

(a) Yeo and Akgerman (1990)
(b) Ghonasgi et al. (1991)

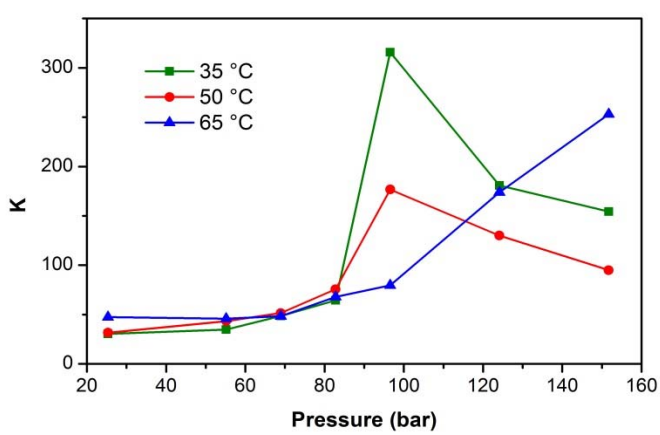

Figure 22: Partitioning coefficients of benzene in water-CO_2 determined in this study.

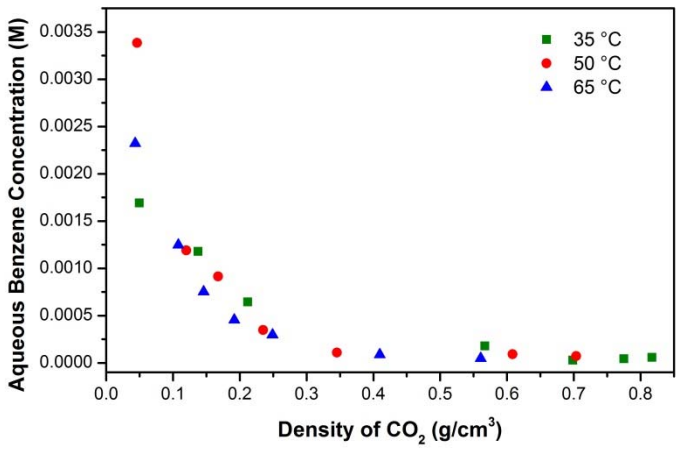

Figure 23: Aqueous benzene concentrations as a function of CO_2 phase density.

4.4 DISCUSSION

For comparative purposes, it is useful to consider methodologies formerly employed for the measurement of partitioning coefficient. Yeo and Akgerman (1990) prepared experimental data for the partitioning coefficient of benzene from saturated water solutions. Samples were mixed in a windowed mixing cell and organic concentrations in each phase were determined by collection of a portion of the CO_2 and water solutions in glass containers. Benzene used for sampling was radiolabeled and concentrations measured via a Beckman liquid scintillation counter (Yeo et al., 1990). Ghonasgi et al. (1991) also mixed samples, in this case well below levels of water saturation, which were mixed with a CO_2 phase in a cell and allowed to equilibrate. In this case, samples from each phase were collected and measured by gas chromatograph to determine benzene concentration (Ghonasgi et al., 1991). When compared to experimental results of other studies, it is apparent that the values measured previously are on the order of 10 times larger than those measured in this work. There may be several contributing factors which influence these measurements. First, as is noted by Ghonasgi et al. (1991), benzene's high volatility makes it a challenging compound to control for measurement via ex situ techniques. In this case, both studies employ ex situ techniques. Loss of benzene via degassing and evaporation between collection from the reaction vessel and analysis may have caused measured benzene concentration in the water phase to be lower than concentrations inside the reaction vessel. To verify reproducibility of samples, K values were collected in triplicate for select conditions. These measurements display deviation of <2%. Detection limits for both the UV and NIR detectors were estimated as 3σ, where σ is taken to be the standard deviation observed in blank measurement. In the NIR, this suggests a detection limit of 1.7×10^{-4} M for benzene. In the UV, detection limit was estimated to be 1.03×10^{-5} M benzene.

Additionally, while initial concentrations of benzene in the water phase were similar for experimental values reported here and those prepared by Ghonasgi et al. (1991), Yeo and Akgerman (1990) measured partitioning values with starting concentrations considerably higher than those reported here. While generally K value is not affected by starting concentrations,

which are much lower than saturation, Yeo et al. (1990) used starting concentrations which approach saturation, which may contribute to discrepancies in measured K values. Such dependence of K values measured experimentally on starting concentration in the aqueous phase was documented by Curren and Burke (1998) in their study of partitioning of pentachlorophenol.

For comparative purposes, the partitioning coefficient of toluene at 50°C and 96.53 bar was measured, and found to be 245.1. As is noted by Timko et al. (2004), experimental values suggest a correlation between water solubility and K value for organics which would indicate a K value for toluene greater than that of benzene, which is observed here. This trend is not observed in other experimental data sets, and is accounted for here by high levels of uncertainty observed in previously collected data (Timko et al., 2004). When compared to toluene partitioning coefficients measured by Yeo and Akgerman (1990) at 45°C and 93.7 bar, again dramatically higher K values (on the order of approximately 9 times greater than values measured here) were evident, which may be explained by the same conditions discussed for benzene, particularly the high starting concentration, in this case, 91.7% saturation in the water phase.

In the course of data collection, several potential shortfalls for the system reported here were encountered. Most impactful of these shortfalls was the detection limit of the UV detector employed in the water phase measurement loop. In order to maintain dilute starting concentrations to limit impact of concentration on K value, organics of exceptionally low solubility (< approximately 0.45 g/L) cannot be measured. However, this issue would be easily remedied by implementation of a detector with longer path length or use of a more sensitive measurement technique such as fluorescence spectroscopy for compounds such as poly-aromatic hydrocarbons or other compounds which exhibit fluorescence. Additionally, as was mentioned previously, formation of gas pockets in the recirculation loop and subsequent interruption of sampling in the UV cell occasionally made water phase data unusable. Bubble formation, in some cases, was eradicated by cycling the HPLC pump several times, and was most problematic only at higher pressure data points. Additionally, careful priming of the circulation loop appeared to generally prevent any gas pockets from forming.

Table 10 shows concentration values for a theoretical system of equal volumes water and CO_2 to provide comparisons between experimental data as collected by Ghonasgi et al. (1991) and those values reported here. By considering this system, K values collected here would suggest a considerably higher concentration of benzene left dissolved in the water phase (approximately 5.5 times greater). However, due to the much higher relative benzene concentration in the CO_2 phase, the differences in CO_2 phase concentration are only approximately 2%. This also suggests that the closing of mass balance may be misleading when used as a measure for accuracy of partitioning coefficient measurement. For example, if the aforementioned theoretical system was considered, an absence of less than 2% of the total benzene, which is missing from the aqueous phase, is enough to account for the discrepancies in measured K values for those reported here and those reported in other studies.

Table 10: Calculated Benzene Concentrations for a Theoretical System of Equal Volumes H_2O and CO_2

Parameter	Ghonasgi et al. (1991)	This Work[(a)]
Conc CO_2	0.0063759	0.0062624
Conc H_2O	0.0000252	0.0001387
K	981.8215684	176.6993306

(a) Conditions: 50°C, 94.0 bar.

5. REFERENCES

Akinlua, A.; Torto, N.; Ajayi, T. R. Supercritical fluid extraction of aliphatic hydrocarbons from Niger Delta sedimentary rock. *J. Supercrit. Fluids* **2008,** *45*, 57–63.

Anitescu, G.; Tavlarides, L. L. Supercritical extraction of contaminants from soils and sediments. *J. Supercrit. Fluids* **2006,** *38*, 167–180.

Apps, J. A.; Zheng, L.; Zhang, Y.; Xu, T.; Birkholzer, J. T. Evaluation of Potential Changes in Groundwater Quality in Response to CO_2 Leakage from Deep Geologic Storage. *Transp. Porous Media* **2010,** *82*, 215–246.

Aronson, D.; Citra, M.; Shuler, K.; Printup, H.; Howard, P. H. Aerobic Biodegradation of Organic Chemicals in Environmental Media: A Summary of Field and Laboratory Studies. [Online] 1999. http://www.epa.gov/osw/hazard/wastetypes/wasteid/hwirwste/pdf/risk/reports/s0549.pdf (accessed March 2013).

Bachu, S. Sequestration of CO_2 in geological media: Criteria and approach for site selection in response to climate change. *Energy Convers. Manage.* **2000,** *41*, 953–970. DOI: 10.1016/S0196-8904(99)00149-1.

Bachu, S.; Adams, J. J. Sequestration of CO_2 in geological media in response to climate change: capacity of deep saline aquifers to sequester CO_2 in solution. *Energy Convers. Manage.* **2003,** *44*, 3151–3175.

Benson, S. M.; Cole, D. R. CO_2 Sequestration in Deep Sedimentary Formations. *Elements* **2008,** *4*, 325–331.

Benson, S. M.; Surles, T. Carbon dioxide capture and storage: An overview with emphasis on capture and storage in deep geological formations. *Proc. IEEE* **2006,** *94*, 1795–1805.

Blunt, M.; Fayers, F. J.; Orr, F. M. Carbon-Dioxide in Enhanced Oil-Recovery. *Energy Convers. Manage*. **1993,** *34*, 1197–1204.

Bondor, P. L. Applications of Carbon-Dioxide in Enhanced Oil-Recovery. *Energy Convers. Manage*. **1992,** *33*, 579–586.

Brudi, K.; Dahmen, N.; Schmieder, H. Partition coefficients of organic substances in two-phase mixtures of water and carbon dioxide at pressures of 8 to 30 MPa and temperatures of 313 to 333 K. *J. Supercrit. Fluids* **1996,** *9*, 146–151.

Burant, A.; Lowry, G. V.; Karamalidis, A. K. Partitioning Behavior of Organic Contaminants in Carbon Storage Environments: A Critical Review. *Environ. Sci. Technol*. **2013,** *47*, 37–54.

Cabbar, H. C.; Bostanci, A. Moisture effect on the transport of organic vapors in sand. *J. Hazard. Mater*. **2001,** *B82*, 313–322.

Chrastil, J. Solubility of solids and liquids in supercritical gases. *J. Phys. Chem*. **1982,** *86*, 3016–3021.

Curren, M. S.; Burk, R. C. Supercritical fluid extraction of acidic, polar solutes from aqueous matrices: Partitioning data for pentachlorophenol between carbon dioxide and water. *J. Chem. Eng. Data* **1998,** *43*, 978–982.

da Costa, M. A. F.; da Costa, M. F. B. Benzene: A public health matter. *Interciencia* **2002,** *27*, 201–204.

EPA. *2012 Edition of the Drinking Water Standards and Health Advisories*; EPA 822-S-12-001; U.S. Environmental Protection Agency, Office of Water, Washington, DC, 2012.

Fahrner, S.; Schafer, D.; Dethlefesen, F; Dahmke, A. Reactive modelling of CO_2 intrusion into freshwater aquifers: Current requirements, approaches and limitations to account for temperature and pressure effects. *Environ. Earth Sci.* **2012,** *67*, 2269–2283.

Fonseca, J. M. S.; Dohrn, R.; Peper, S. High-pressure fluid-phase equilibria: Experimental methods and systems investigated (2005-2008). *Fluid Phase Equilib*. **2011,** *300*, 1–69.

Galbraith, D.; Gross, S.A.; Paustenbach, D. Benzene and human health: A historical review and appraisal of associations with various diseases. *Crit. Rev. Toxicol*. **2010,** *40*, 1–46.

Ghonasgi, D.; Gupta, S.; Dooley, K. M.; Knopf, F. C. Supercritical CO_2 Extraction of Organic Contaminants from Aqueous Streams. *Aiche J*. **1991,** *37*, 944–950.

Godec, M.; Kuuskraa, V.; Van Leeuwen, T.; Melzer, L. S.; Wildgust, N. CO_2 Storage in Depleted Oil Fields: The Worldwide Potential for Carbon Dioxide Enhanced Oil Recovery. In *10th International Conference on Greenhouse Gas Control Technologies*. Gale, J.; Hendriks, C.; Turkenberg, W., Eds.; Elsevier Science B.V.: Amsterdam, 2011; pp 2162–2169.

Goss, K. U. The air/surface adsorption equilibrium of organic compounds under ambient conditions. *Crit. Rev. Environ. Sci. Technol.* **2004,** *34*, 339–389.

Hawkes, C. D.; Bachu, S.; McLellan, P. J. Geomechanical factors affecting geological storage of CO_2 in depleted oil and gas reservoirs. *J. Can. Pet. Technol*. **2005,** *44*, 52–61.

Hawthrone, S. B.; Hegvik, K. M.; Yang, Y.; Miller, D. Determination of heavy hydrocarbon contamination using supercritical fluid extraction with infrared detection. *Fuel* **1994,** *73*, 1876–1879.

Huff, J. Benzene-induced cancers: Abridged history and occupational health impact. *Int. J. Occup. Environ. Health* **2007,** *13*, 213–221.

Jaffé, R.; Diaz, D.; Fruton, K. G.; Lafargue, E. High temperature supercritical carbon dioxide extractions of geological samples: Effects and contributions from the sample matrix. *Appl. Geochem.* **2000,** *15*, 79–89.

Jaffé, R.; Diaz, D.; Haiji, N.; Chen, L.; Eckardt, C.; Furton, K. G. Hydrocarbon speciation in ancient sediments studied by stepwise high-temperature supercritical carbon dioxide extraction. *Org. Geochem*. **1997,** *26*, 59–65.

Jang, W. Y.; Aral, M. M. Density-driven transport of volatile organic compounds and its impact on contaminated groundwater plume evolution. *Transp. Porous Med*. **2007,** *67*, 353–374.

Joo, J. C.; Song, M. S.; Kim, J. K. Sorption of nonpolar neutral organic compounds to low-surface-area metal (hydr)oxide- and humic acid-coated model aquifer sands. *J. Environ. Sci. Health., Part A* **2012,** *47*, 909–918.

Karasek, P.; Pol, J.; Planeta, J.; Roth, M.; Vejrosta, J.; Wicar, S. Partition coefficients of environmentally important phenols in a supercritical carbon dioxide-water system from

cocurrent extraction without analysis of the compressible phase. *Anal. Chem*. **2002,** *74*, 4294–4299.

Kharaka, Y. K.; Campbell, P.; Thomas, R. B. Environmental Impacts of Geologic Sequestration of CO_2: Mobilized Toxic Organic Compounds. In *International Symposium on Isotopes in Hydrology, Marine Ecosystems, and Climate Change Studies*, International Atomic Energy Agency, Monaco, March 29, 2011.

Kharaka, Y. K.; Cole, D. R.; Hovorka, S. D.; Gunter, W. D.; Knauss, K. G.; Freifeld, B. M. Gas-Water-Rock Interactions in Frio Formation Following CO_2 Injection: Implications for the Storage of Greenhouse Gases in Sedimentary Basins. *Geology* **2006,** *34*, 577–580.

Kharaka, Y. K.; Thordsen, J. J.; Hovorka, S. D.; Nance, H. S.; Cole, D. R.; Phelps, T. J.; Knauss, K. G. Potential Environmental Issues of CO_2 Storage in Deep Saline Aquifers: Geochemical Results from the Frio-I Brine Pilot Test, Texas, USA. *Appl. Geochem.* **2009,** *24*, 1106–1112.

Kharaka, Y. K.; Campbell, P.; Thorden, J. J.; Thomas, P. B.; Cole, D. R.; Hovorka, S. D. Geologic storage of carbon dioxide: Potential environmental impacts of CO_2-organic interactions. *Geochm. Cosmoschim. Acta* **2010a,** *74*, A511-A511.

Kharaka, Y. K.; Thordsen, J. J.; Kakouros, E.; Ambats, G.; Herkelrath, W. N.; Beers, S. R.; Birkholzer, J. T.; Apps, J. A.; Spycher, N. F.; Zheng, L.; Trautz, R. C.; Rauch, H. W.; Gullickson, K. S. Changes in the Chemistry of Shallow Groundwater Related to the 2008 Injection of CO_2 at the ZERT Field Site, Bozeman, Montana. *Environ. Earth Sci.* **2010b,** *60*, 273–284.

Koel, M.; Ljovin, S. Supercritical carbon dioxide extraction of Estonian oil shale. *Oil Shale* **2000,** *17*, 225–232.

Kolak, J. J.; Burruss, R. C. Geochemical investigation of the potential for mobilizing non-methane hydrocarbons during carbon dioxide storage in deep coal beds. *Energy Fuels* **2006,** *20*, 566–574.

Kometani, N.; Takemiya, K.; Yonezawa, Y.; Amita, F.; Kajimoto, O. UV spectral shift of benzene in sub- and supercritical water. *Chem. Phys. Lett*. **2004,** *394*, 85–89.

Kordikowski, A.; Robertson, D. G.; Aguiar-Ricardo, A. I.; Popov, V. K.; Howdle, S. M.; Poliakoff, M. Probing Vapor/Liquid Equilibria of Near-Critical Binary Gas Mixtures by Acoustic Measurements. *J. Phys. Chem*. **1996,** *100*, 9522–9526.

Lin, J. H.; Chou, M. S. Temperature effects on Henry's law constants for four VOCs in air-activated sludge systems. *Atmos. Environ.* **2006,** *40*, 2469–2477.

Mackay, D.; Shiu, W. Y. A critical review of Henry's law constants for chemicals of environmental interest. *J. Phys. Chem. Ref. Data.* **1981,** *10*, 1175–1199.

McKay, J. F.; Chong, S. Supercritical fluid extraction of oil from eastern oil shales. In *1983 Eastern Oil Shale Symposium*, Lexington, KY, Nov 13–16, 1983; pp 235–239.

Mathieu, P. *The IPCC special report on carbon dioxide capture and storage*; National Technical University Athens: Zografou, 2006; pp 1611–1617.

McHugh, M. A.; Krukonis, V. J. *Supercritical fluid extraction. Principles and practice*; Butterworth-Heinemann: Boston, MA, 1986; pp 448.

Monin, J. C.; Barth, D.; Perrut, M.; Espitalie, M.; Durand, B. Extraction of hydrocarbons from sedimentary rocks by supercritical carbon dioxide. Organic Geochemistry. **1988,** *13*, 1079–1086.

Montgomery, J. H.; Welkom, L. M. *Groundwater Chemicals Desk Reference*. Lewis Publishers, Inc., Boca Raton, FL, 1990.

Morgenstern, D. A.; LeLacheur, R. M.; Morita, D. K.; Borkowsky, S. L.; Feng, S.; Brown G. H.; Luan, L.; Gross, M. F.; Burk, M. J.; Tumas, W. Supercritical Carbon Dioxide as a Substitute Solvent for Chemical Synthesis and Catalysis. In *Green Chemistry*; American Chemical Society, 1996; pp 132–151.

Okamoto, I.; Li, X.; Ohsumi, T. Effect of supercritical CO_2 as the organic solvent on cap rock sealing performance for underground storage. *Energy* **2005,** *30*, 2344–2351.

Olukcu, N.; Yanik, J.; Saglam, M.; Yuksel, M.; Karaduman, M. Solvent effect on the extraction of Beypazari oil shale. *Energy Fuels* **1999,** *13*, 895–902.

Peng, D.; Robinson, D. B. New 2-Constant Equation of State. *Ind. Eng. Chem. Fundam*. **1976,** *15*, 59–64.

Piwoni, M. D.; Banerjee, P. Sorption of Volatile Organic Solvents from Aqueous Solution onto Subsurface Solids. *J. Contam. Hydrol*. **1989,** *4*, 163–179.

Qin, K.; Wang, G.; Jia, S. Chemical structure investigation of Maoming oil shale kerogen by supercritical gas extraction. *Energy Source* **1984,** *7*, 237–255.

Rivett, M. O.; Wealthall, G. P.; Dearden, R. A.; McAlary, T. A. Review of unsaturated-zone transport and attenuation of volatile organic compound (VOC) plumes leached from shallow source zones. *J. Contam. Hydrol*. **2011,** *123*, 130–156.

Ruiz, J.; Bilbao, R.; Murillo, M. B. Adsorption of different VOC onto soil minerals from gas phase: Influence of mineral, type of VOC, and air humidity. *Environ. Sci. Technol*. **1998,** *32*, 1079–1084.

Scherf, A-K.; Zetzl, C.; Smirnova, I.; Zettlitzer, M.; Vieth-Hillebrand, A.; CO2SINK-Group. Mobilisation of Organic Compounds from Reservoir Rocks Through the Injection of CO_2 – Comparison of Baseline Characterization and Laboratory Experiments. *Energy Procedia* **2011,** *4*, 4524–4531.

Schroth, M. H.; Ahearn, S. J.; Selker, J. S.; Istok, J. D. Characterization of Miller-similar silica sands for laboratory hydrologic studies. *Soil Sci. Soc. Am. J*. **1996,** *60*, 1331–1339.

Schwarzenbach, R. P.; Westall, J. Transport of Nonplar Organic Compounds from Surface Water to Groundwater. Laboratory Sorption Studies. *Environ. Sci. Technol.* **1981,** *15*, 1360–1367.

Schwarzenbach, R. P.; Gschwend, P. M.; Imboden, D. M. *Environmental Organic Chemistry*, 2nd Ed.; John Wiley & Sons, Inc.: Hoboken, NJ, 2003.

Spycher, N.; Pruess, K.; Ennis-King, J. CO_2-H_2O mixtures in the geological sequestration of CO_2. I. Assessment and calculation of mutual solubilities from 12 to 100 degrees C and up to 600 bar. *Geochim. Cosmochim. Acta* **2003,** *67*, 3015–3031.

Takebayashi, Y.; Sagisaka, M.; Sue, K.; Yoda, S.; Hakuta, Y.; Furuya, T. Near-Infrared Spectroscopic Study of a Water-in-Supercritical CO_2 Microemulsion as a Function of the Water Content. *J. Phys. Chem. B* **2011,** *115*, 6111–6118.

Thomson, N. R.; Sykes, J. F.; Van Vliet, D. A numerical investigation into factors affecting gas and aqueous phase plumes in the subsurface. *J. Contam. Hydrol.* **1997,** *28*, 39–70.

Timko, M. T.; Nicholson, B. F.; Steinfeld, J. I.; Smith, K. A.; Tester, J. W. Partition coefficients of organic solutes between supercritical carbon dioxide and water: Experimental measurements and empirical correlations. *J. Chem. Eng. Data* **2004,** *49*, 768–778.

White, C. M.; Strazisar, B. R.; Granite, E. J.; Hoffman, J. S.; Pennline, H. W. Separation and Capture of CO_2 from Large Stationary Sources and Sequestration in Geological Formations--Coalbeds and Deep Saline Aquifers. *J. Air Waste Manage. Assoc.* **2003,** *53*, 645–715.

White, M. D.; McGrail, B. P. *STOMP, Subsurface Transport Over Multiple Phases, Version 1.0, Addendum: ECKEChem, Equilibrium-Conservation-Kinetic Equation Chemistry and Reactive Transport*; PNNL-15482; Pacific Northwest National Laboratory: Richland, WA, 2005.

White, M. D.; Oostrom, M. *STOMP: Subsurface Transport Over Multiple Phases, Version 4.0, User's Guide*; PNNL-15782; Pacific Northwest National Laboratory: Richland, Washington, 2006; p 120.

Wilbur, S.; Wohlers, D.; Paikoff, S.; Keith, L. S.; Faroon, O. ATSDR evaluation of health effects of benzene and relevance to public health. *Toxicol. Ind. Health* **2008,** *24*, 263–398.

Workman, J.; Weyer, L. *Practical Guide to Interpretive Near-Infrared Spectroscopy*; CRC Press, Taylor & Francis Group: Boca Raton, FL, 2007.

Xu, T.; Apps, J. A.; Birkholzer, J. T. Contamination of groundwater by hazardous inorganic chemical constituents through induced acidification due to CO_2 leakage from a storage formation. In *Abstract in Proceedings 6th Annual Conference on Carbon Capture and Sequestration*, Pittsburgh, PA, May 2007.

Yeo, S .D.; Akgerman, A. Supercritical Extraction of Organic Mixtures from Aqueous-Solutions. *Aiche J*. **1990,** *36*, 1743–1747.

Zheng, L.; Spycher, N.; Birkholzer, J.; Xu, T.; Apps, J.; Kharaka, Y. *Modeling Studies on the Transport of Benzene and H_2S in CO_2-Water Systems*; LBNL-4339E; Lawrence Berkeley National Laboratory: Berkeley, CA, 2010.

Zheng, L. G.; Spycher, N.; Birkholzer, J.; Xu, T. F.; Apps, J.; Kharaka, Y. On modeling the potential impacts of CO_2 sequestration on shallow groundwater: Transport of organics and co-injected H_2S by supercritical CO_2 to shallow aquifers. *Int. J. Greenh. Gas Control* **2013,** *14*, 113–127.

Zhong, L.; Cantrell, K.; Mitroshkov, A.; Shewell, J. Mobilization and Transport of Organic Compounds from Reservoir Rock and Caprock in Geological Carbon Sequestration Sites. *Environ. Earth Sci.* **2014**, 71, 4261–4272.

NRAP is an initiative within DOE's Office of Fossil Energy and is led by the National Energy Technology Laboratory (NETL). It is a multi-national-lab effort that leverages broad technical capabilities across the DOE complex to develop an integrated science base that can be applied to risk assessment for long-term storage of carbon dioxide (CO_2). NRAP involves five DOE national laboratories: NETL, Lawrence Berkeley National Laboratory (LBNL), Lawrence Livermore National Laboratory (LLNL), Los Alamos National Laboratory (LANL), and Pacific Northwest National Laboratory (PNNL).

Technical Leadership Team

Diana Bacon
Lead, Groundwater Protection Working Group
Pacific Northwest National Laboratory
Richmond, WA

Jens Birkholzer
LBNL Technical Coordinator
Lawrence Berkeley National Laboratory
Berkeley, CA

Grant Bromhal
Technical Director, NRAP
Lead, Reservoir Performance Working Group
Office of Research and Development
National Energy Technology Laboratory
Morgantown, WV

Chris Brown
PNNL Technical Coordinator
Pacific Northwest National Laboratory
Richmond, WA

Susan Carroll
LLNL Technical Coordinator
Lawrence Livermore National Laboratory
Livermore, CA

Tom Daley
Lead, Strategic Monitoring Working Group
Lawrence Berkeley National Laboratory
Berkeley, CA

Robert Dilmore
NETL Technical Portfolio Lead
Office of Research and Development
National Energy Technology Laboratory
Pittsburgh, PA

Nik Huerta
Lead, Migration Pathways Working Group
Office of Research and Development
National Energy Technology Laboratory
Albany, OR

Rajesh Pawar
LANL Technical Coordinator
Lead, Systems/Risk Modeling Working Group
Los Alamos National Laboratory
Los Alamos, NM

Tom Richard
Deputy Technical Director, NRAP
The Pennsylvania State University
State College, PA

Josh White
Lead, Induced Seismicity Working Group
Lawrence Livermore National Laboratory
Livermore, CA

Sean Plasynski
Director
Strategic Center for Coal
National Energy Technology Laboratory
U.S. Department of Energy

John Wimer
Director
Office of Coal and Power R&D
National Energy Technology Laboratory
U.S. Department of Energy

Traci Rodosta
Technology Manager
Carbon Storage
National Energy Technology Laboratory
U.S. Department of Energy

Mark Ackiewicz
Director
Division of Carbon Capture and Storage
Office of Fossil Energy
U.S. Department of Energy

NRAP Executive Committee

Cynthia Powell
Director
Office of Research and Development
National Energy Technology Laboratory
U.S. Department of Energy

Alain Bonneville
Laboratory Fellow
Pacific Northwest National Laboratory

Donald DePaolo
Chair, NRAP Executive Committee
Associate Laboratory Director
Energy and Environmental Sciences
Lawrence Berkeley National Laboratory

Melissa Fox
Program Manager
Applied Energy Programs
Los Alamos National Laboratory

Roger Aines
Chief Energy Technologist
Lawrence Livermore National
Laboratory

Grant Bromhal
Technical Director, NRAP
Office of Research and Development
National Energy Technology Laboratory

NRAP Technical Report Series